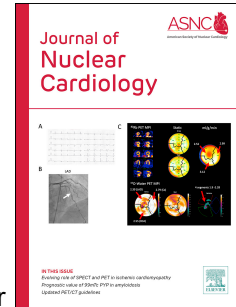


# Journal Pre-proof

Cardiovascular PET imaging of fibroblast activation A review of the current literature

Krithika Loganath, Neil Craig, Anna Barton, Shruti Joshi, Constantinos Anagnostopoulos, Paola Anna Erba, Andor W.J.M. Glaudemans, Antti Saraste, Jan Bucerius, Mark Lubberink, Olivier Gheysens, Ronny R. Buechel, Gilbert Habib, Oliver Gaemperli, Alessia Gimelli, Fabien Hyafil, David E. Newby, Riemer H.J.A. Slart, Marc R. Dweck



PII: S1071-3581(24)00808-0

DOI: <https://doi.org/10.1016/j.nuclcard.2024.102106>

Reference: YMNC 102106

To appear in: *Journal of Nuclear Cardiology*

Received Date: 10 May 2024

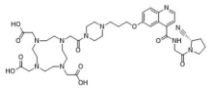
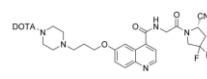
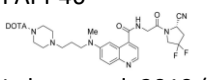
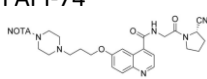
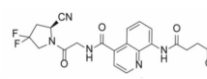
Revised Date: 22 November 2024

Accepted Date: 29 November 2024

Please cite this article as: Loganath K, Craig N, Barton A, Joshi S, Anagnostopoulos C, Erba PA, Glaudemans AWJM, Saraste A, Bucerius J, Lubberink M, Gheysens O, Buechel RR, Habib G, Gaemperli O, Gimelli A, Hyafil F, Newby DE, Slart RHJA, Dweck MR, Cardiovascular PET imaging of fibroblast activation A review of the current literature *Journal of Nuclear Cardiology*, <https://doi.org/10.1016/j.nuclcard.2024.102106>.

This is a PDF file of an article that has undergone enhancements after acceptance, such as the addition of a cover page and metadata, and formatting for readability, but it is not yet the definitive version of record. This version will undergo additional copyediting, typesetting and review before it is published in its final form, but we are providing this version to give early visibility of the article. Please note that, during the production process, errors may be discovered which could affect the content, and all legal disclaimers that apply to the journal pertain.

© 2024 The Author(s). Published by Elsevier Inc. on behalf of American Society of Nuclear Cardiology.

Name	Chelator	Healthy myocardial uptake and internalisation	Hepatobiliary excretion	Tissue retention
FAPI-02  Loktev et al, 2018 (34)	DOTA	Medium	High	Low
FAPI-04  Lindner et al, 2018 (29)	DOTA	Medium	Medium	Medium
FAPI-46  Loktev et al, 2019 (48) Meyer et al, 2020 (49)	DOTA	Medium	Medium	High
FAPI-74  Giesel et al, 2021 (32) Lindner et al, 2021 (113)	NOTA	High	Low	High
ONCOFAP  Millul et al, 2021 (114) Backhaus et al, 2022 (115)	NOTA and DOTA	Low	Low	High

<b>Myocardial infarction</b>					
<b><i>Preclinical studies</i></b>					
<b>Title</b>	<b>Model</b>	<b>Tracer</b>	<b>Imaging modality</b>	<b>Key results</b>	
Varasteh et al (59)	Murine	<sup>68</sup> Ga-FAPI	PET-CT, autoradiography	<ul style="list-style-type: none"> <li>• Peak radiotracer uptake observed at 6 days post MI with return to baseline by 14 days</li> <li>• Peri-infarct regions demonstrated more intense uptake than infarct regions</li> <li>• No remote myocardial uptake up to 14 days</li> <li>• FAP expression confirmed in areas on <sup>68</sup>Ga-FAPI uptake on immunofluorescence</li> <li>• FAP+ cells were observed 3 and 8 times more in the border zones than in infarct and remote myocardium, respectively</li> </ul>	
Qiao et al, 2022 (60)	Rat	<sup>68</sup> Ga-FAPI	PET-CT, Autoradiography, Immunofluorescenc, H&E staining	<ul style="list-style-type: none"> <li>• Peak radiotracer uptake in infarcted myocardium with gradual decline until day 35, where uptake was similar to the sham-operated group</li> <li>• No significant remote <sup>68</sup>Ga-FAPI uptake was noted up to 35 days</li> <li>• Higher uptake demonstrated at the border zones on autoradiography</li> </ul>	
<b><i>Clinical studies</i></b>					
<b>Title</b>	<b>Cohort and design</b>	<b>Tracer</b>	<b>Imaging modality</b>	<b>Key points</b>	<b>Correlation with imaging and serum biomarkers</b>

Diekmann et al (63)	12 STEMI patients, Prospective	<sup>68</sup> Ga-FAPI	PET-CT, SPECT, CMR	<ul style="list-style-type: none"> <li>Significant <sup>68</sup>Ga-FAPI uptake in the infarct, extending into the peri-infarct zones</li> </ul>	<ul style="list-style-type: none"> <li><sup>68</sup>Ga-FAPI uptake areas exceeds infarct areas identified on SPECT and CMR LGE imaging</li> </ul>
Kessler et al (65)	5 STEMI and 5 NSTEMI patients, Prospective	<sup>68</sup> Ga-FAPI	PET-CT	<ul style="list-style-type: none"> <li>All patients had significant <sup>68</sup>Ga-FAPI uptake in the myocardium</li> <li>A complete to partial concordance was observed of visual <sup>68</sup>Ga-FAPI myocardial uptake and areas supplied by the culprit vessel</li> </ul>	<ul style="list-style-type: none"> <li><sup>68</sup>Ga-FAPI uptake volume was positively correlated with peak CK level and negatively correlated with LVEF</li> </ul>
Xie et al (62)	14 STEMI patients and 14 healthy volunteers, Prospective	<sup>68</sup> Ga-FAPI	PET-CT and CMR	<p>14 patients post STEMI</p> <ul style="list-style-type: none"> <li>Significant <sup>68</sup>Ga-FAPI uptake was observed over infarct zones and beyond</li> <li>Baseline TBR<sub>max</sub> inversely correlated with LV function at 7 weeks</li> </ul>	<ul style="list-style-type: none"> <li>Areas of <sup>68</sup>Ga-FAPI uptake extended beyond LGE on CMR</li> </ul>
Zhang et al (64)	26 STEMI patients, Prospective	<sup>68</sup> Ga-FAPI	PET-MR	<ul style="list-style-type: none"> <li>Increased <sup>68</sup>Ga-FAPI volumes and TBR<sub>max</sub> at baseline correlated with reduced LVEF at 1 year</li> <li>Patients who had late LV remodelling ( increase in LVESV &gt;10% from baseline) had a higher</li> </ul>	<ul style="list-style-type: none"> <li>No significant correlation between <sup>68</sup>Ga-FAPI volumes and serum biomarkers such as NT-proBNP and serum troponin I.</li> <li>Baseline <sup>68</sup>Ga-FAPI predicted late LV remodelling better</li> </ul>

				baseline <sup>68</sup> Ga-FAPI volume	than LGE% and LGE volume on CMR
--	--	--	--	--	------------------------------------

Journal Pre-proof

<b>Myocardial diseases</b>					
<b><i>Preclinical studies</i></b>					
<b>Title</b>	<b>Condition</b>	<b>Model</b>	<b>Tracer</b>	<b>Imaging Modality</b>	<b>Key points</b>
Wang et al (66)	Pressure-overload	Rat	<sup>68</sup> Ga-FAPI	PET-CT, PET-MR, Echocardiography, Immunohistochemistry	<ul style="list-style-type: none"> <li>• Areas of increased <sup>68</sup>Ga-FAPI uptake corresponded with areas of myocardial hypertrophy on CMR</li> <li>• Early <sup>68</sup>Ga-FAPI uptake at 4 weeks corresponded to a reduced LVEF at 8 weeks</li> <li>• Increased myocardial <sup>68</sup>Ga-FAPI uptake in areas corresponding FAP expression on immunohistochemistry</li> </ul>
Sun et al (67)	HFpEF	Rat	<sup>18</sup> F-AIF-FAPI	PET-CT, Immunohistochemistry, Masson staining	<ul style="list-style-type: none"> <li>• Increased <sup>18</sup>F-AIF-FAPI uptake in the LV myocardium in rats corresponded to post-mortem areas of FAP+ cells and interstitial and vascular fibrosis</li> </ul>
Song et al (68)	HFrEF	Murine	<sup>68</sup> Ga-FAPI	PET-CT	<ul style="list-style-type: none"> <li>• A positive correlation was seen between baseline LV myocardial <sup>68</sup>Ga-FAPI uptake and decline in LV contractility and increased LV dilatation at 28 days</li> </ul>
Wei et al (69)	Anthracycline-induced cardiotoxicity	Rat	<sup>68</sup> Ga-FAPI	PET-CT, Echocardiography, Immunohistochemistry, Masson staining	<ul style="list-style-type: none"> <li>• <sup>68</sup>Ga-FAPI uptake was significantly higher in rats with cardiotoxicity compared to control rats at weeks 3 and 6 although no significant change in LVEF was seen between groups</li> <li>• Enalapril treatment for 3 weeks reduced the intensity of <sup>68</sup>Ga-FAPI uptake, preserved LVEF and reduced myocardial fibrosis on Masson staining</li> </ul>

<b><i>Clinical studies</i></b>						
<b>Title</b>	<b>Condition</b>	<b>Cohort and design</b>	<b>Tracer</b>	<b>Imaging Modality</b>	<b>Key points</b>	<b>Correlation with imaging and serum biomarkers</b>
Wang et al (72)	Multiple non-ischaemic cardiomyopathies	29 patients, Prospective	<sup>68</sup> Ga-FAPI	PET-CT, echocardiography	<ul style="list-style-type: none"> <li>• 22 of the 29 scanned patients had heterogenous LV myocardial FAPI uptake</li> <li>• 10 patients had RV myocardial FAPI uptake across a spectrum of aetiologies</li> </ul>	<ul style="list-style-type: none"> <li>• SUV<sub>max</sub> correlated significantly with LVEDD on echocardiography</li> </ul>
Song et al (68)	HFrEF	7 patients, 20 participants without cardiac disease, Prospective	<sup>68</sup> Ga-FAPI	PET-CT, <sup>13</sup> N-NH <sub>3</sub> perfusion scan	<ul style="list-style-type: none"> <li>• Significantly elevated LV myocardial <sup>68</sup>Ga-FAPI uptake was seen in patients compared to healthy volunteers</li> </ul>	<ul style="list-style-type: none"> <li>• Areas of <sup>68</sup>Ga-FAPI uptake did not correspond with areas of reduced perfusion on <sup>13</sup>N-NH<sub>3</sub> myocardial perfusion scan</li> </ul>
Wang et al (71)	HCM	50 patients with HCM vs 20 healthy volunteers, Prospective	<sup>18</sup> F-AIF-FAPI	PET-CT, CMR (without gadolinium)	<ul style="list-style-type: none"> <li>• Significantly higher LV myocardial <sup>18</sup>F-AIF-FAPI uptake in patients compared to healthy volunteers</li> <li>• 32 (64%) patients had increased <sup>18</sup>F-AIF-FAPI uptake in the RV myocardium and 4</li> </ul>	<ul style="list-style-type: none"> <li>• Increased <sup>18</sup>F-AIF-FAPI uptake was seen in all hypertrophied segments but also in non-hypertrophied segments in 84% of patients</li> <li>• <sup>18</sup>F-AIF-FAPI had a positive relationship</li> </ul>

					<p>(8%) had significant <math>^{18}\text{F}</math>-AIF-FAPI uptake in the atria, 3 of whom had AF.</p> <ul style="list-style-type: none"> <li>Increased <math>^{18}\text{F}</math>-AIF-FAPI uptake positively correlated with the 5-year sudden cardiac death score and risk of malignant arrhythmia</li> </ul>	with NT-proBNP and hs-cTnI and negative relationship with LVEF
Chen et al (74)	Chronic thromboembolic pulmonary hypertension	13 patients with CTEPH, prospectively recruited	$^{68}\text{Ga}$ -FAPI	PET-CT, CMR, RHC	<ul style="list-style-type: none"> <li>10 of the 13 patients demonstrated significant free RV wall <math>^{68}\text{Ga}</math>-FAPI uptake</li> <li><math>^{68}\text{Ga}</math>-FAPI uptake positively correlated with RV wall thickness and negatively correlated with RVEF</li> </ul>	<ul style="list-style-type: none"> <li>Only 27% of significant RV <math>^{68}\text{Ga}</math>-FAPI uptake corresponded to LGE on CMR</li> <li>No correlation between <math>^{68}\text{Ga}</math>-FAPI uptake and pulmonary haemodynamic parameters on RHC</li> </ul>
Gu et al (75)	Pulmonary arterial hypertension	16 patients with PAH, prospectively recruited	$^{68}\text{Ga}$ -FAPI	PET-CT, echocardiography, RHC	<ul style="list-style-type: none"> <li>12 of the 16 patients had significant RV free wall and insertion point <math>^{68}\text{Ga}</math>-FAPI uptake</li> </ul>	<ul style="list-style-type: none"> <li><math>^{68}\text{Ga}</math>-FAPI uptake correlated with TAPSE on echocardiography</li> <li>No significant correlation between <math>^{68}\text{Ga}</math>-FAPI uptake and pulmonary haemodynamic parameters on RHC</li> </ul>

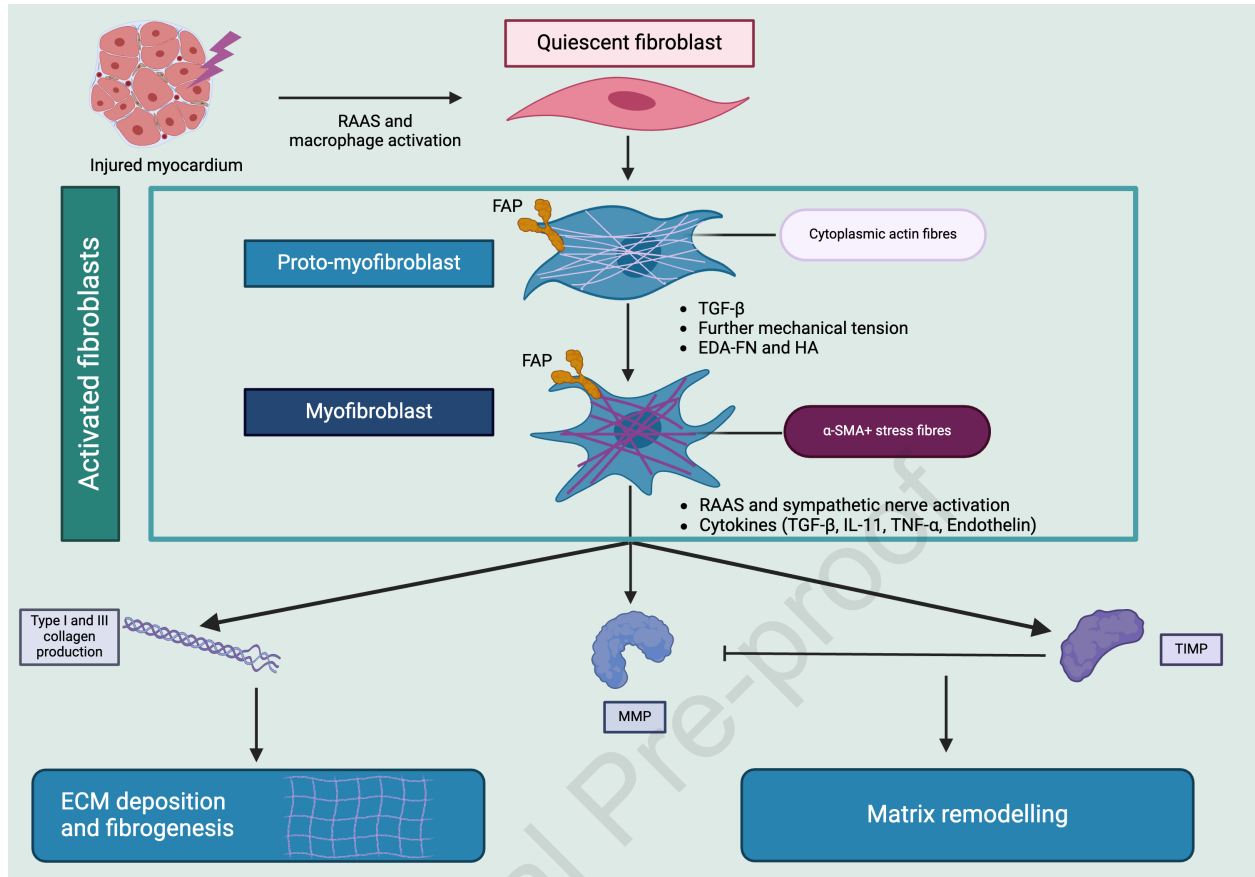
Finke et al (73)	Checkpoint-inhibitor (ICI) associated myocarditis	26 patients who received ICI, 3 with myocarditis, Retrospective analysis	<sup>68</sup> Ga-FAPI	PET-CT, CMR	<ul style="list-style-type: none"> <li>• <sup>68</sup>Ga-FAPI uptake significantly higher in ICI myocarditis patients</li> </ul>	<ul style="list-style-type: none"> <li>• 2/3 patients with ICI had MRI. 1 had globally elevated T1-mapping and another had basal LGE. T2 mapping was normal</li> </ul>
Wang et al (70)	Cardiac AL-amyloidosis	30 patients with AL amyloidosis (27 with cardiac involvement and 3 without) , Prospective	<sup>68</sup> Ga-FAPI	PET-CT, CMR, Echocardiography	<ul style="list-style-type: none"> <li>• 80% of AL CA patients had increased intensity of myocardial <sup>68</sup>Ga-FAPI uptake</li> </ul>	<ul style="list-style-type: none"> <li>• 4 patients with LGE on CMR also had significant <sup>68</sup>Ga-FAPI uptake</li> <li>• FAPI uptake correlated with Mayo stage and NTpro-BNP levels, ECV percentage on CMR and negatively correlated with LVPW thickness and LVEF on CMR</li> </ul>

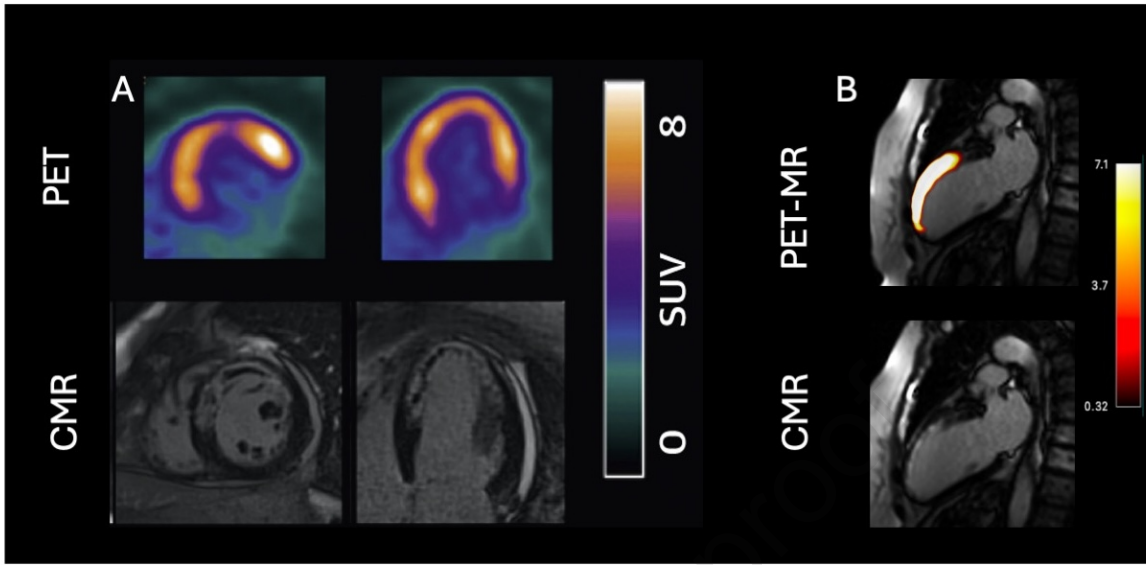
Receptor	Function	Name of drug	Preclinical data		Clinical data		
			Cohort and model	Key points	Cohort and design	Key points	
CTGF Also known as CCN2	Mediates ECM production in pathological states	CTGF-mAb	Pressure-overload, mice(116)	<ul style="list-style-type: none"> <li>Improved LV systolic function</li> <li>Reduced cardiomyocyte hypertrophy in murine models</li> </ul>	Nil		
			DCM, mice (117)	<ul style="list-style-type: none"> <li>Improved LV systolic and diastolic dysfunction</li> </ul>			Nil
			MI, mice (118)	<ul style="list-style-type: none"> <li>Improved 7-day survival</li> <li>Improved LV function</li> <li>No difference in infarct size or 7 week survival</li> </ul>			Nil
Galectin-3	Interacts with aldosterone to promote macrophage infiltration and mediates cardiac fibroblast proliferation	Modified Citrus Protein (MCP)	HF, rats (119)	<ul style="list-style-type: none"> <li>Improved LV function</li> <li>Reduced expression of collagen 1 and 3 genes</li> </ul>	Nil		
			HF, mice (120)	<ul style="list-style-type: none"> <li>Improved LV function</li> <li>Reduction in cardiac hypertrophy and fibrosis when treated in combination with an aldosterone antagonist</li> </ul>			
MicroRNA- 132-3p (miR-132)	Downregulates expression of Forkhead box O3 (FOXO3) which is anti-hypertrophic	Anti-miR-132	Post-MI HFREF, mice (121)	<ul style="list-style-type: none"> <li>Improved LVEF and NT pro-BNP levels</li> <li>Reduction in myocardial interstitial fibrosis on in mice</li> </ul>	Prospective randomised, double-blind, placebo-controlled trial of 28 patients	<ul style="list-style-type: none"> <li>No adverse reactions</li> <li>Combined endpoint of NT pro-BNP reduction of &gt;10% and LVEF increase</li> </ul>	

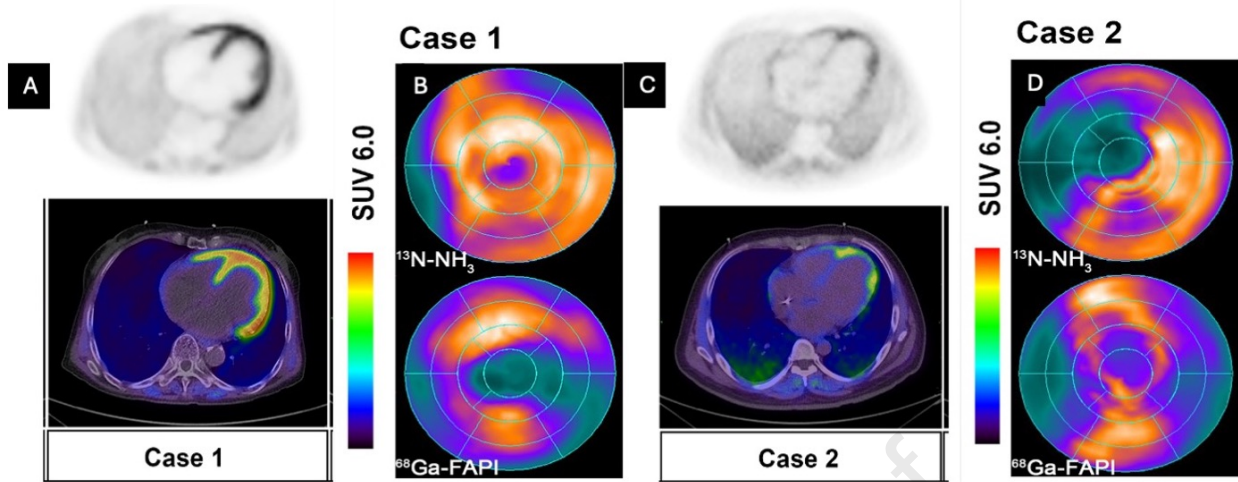
	and suppresses calcium handling and myocardial contractility				with HFREF (LVEF 30-49%) (122)	of >2% was achieved in 79% in the pharmacodynamically active group vs 46% in the inactive group
Renin	Inhibits angiotensin II and promotes angiotensin II-independent reduction in TGF $\beta$ -1 and collagen production	Aliskiren	Pressure-overload, mice (123)	<ul style="list-style-type: none"> <li>Improved LVEF, LVFS and collagen volume</li> </ul>		Nil
TGF- $\beta$	Inhibition of TGF- $\beta$ reduces collagen deposition in the extracellular matrix	Pirfenidone	Pressure-overload, mice (124)		PIROUTTE trial-randomised, double-blind, placebo-controlled trial in 47 HFpEF patients (125)	<ul style="list-style-type: none"> <li>Reduction of ECV and LV mass on CMR</li> <li>26% of treated patients has side effects (nausea, insomnia, rash) although similar to placebo group</li> </ul>
			MI (126)	<ul style="list-style-type: none"> <li>Lower total LV fibrosis</li> <li>Higher LVEF</li> </ul>		

Phosphorylated Smad2 inhibitor	Phosphorylated Smad2, a downstream product of TGF-beta, increases ECM production	FT011	MI, rat (127)	<ul style="list-style-type: none"> <li>Improved LVEF</li> <li>Reduced amount of cardiac fibrosis in non-infarct regions</li> </ul>	Nil	
Matrix metalloproteinase (MMP) inhibitors	MMPs promote the degradation of ECM and adverse myocardial remodelling	PG-116800	Pressure-overload, mice (128)	<ul style="list-style-type: none"> <li>Lower LVEDV and interstitial fibrosis in MMP knockout (KO) mice</li> <li>No difference in LVEF (128)</li> </ul>	Randomised placebo-controlled double-blind trial of 253 post-STEMI HFrEF patients (129)	<ul style="list-style-type: none"> <li>No difference in mortality, cardiac admissions or LVEF</li> <li>Higher incidence of gastrointestinal disturbance and joint stiffness in the treatment group</li> </ul>
			MI, mice (130)	<ul style="list-style-type: none"> <li>MMP-29 KO mice had a lower 7-day survival mostly due to cardiac rupture.</li> <li>LVESD and LVEDD were higher in KO mice than WT, while collagen I and III were lower in KO mice (130)</li> </ul>		
Relaxin	Stimulates fibroblast differentiation and collagen deposition as well as promoting	Seralaxin	MI, mice (131)	<ul style="list-style-type: none"> <li>Lower LVEDP</li> <li>Reduced collagen volume in infarct and border regions</li> <li>No significant difference in LVEF</li> </ul>	RELAX-AHF trial- a randomised placebo-controlled trial of Seralaxin in 1161 acute	<ul style="list-style-type: none"> <li>Improved patient-reported dyspnoea but no difference in days alive out of hospital up to 60 days</li> </ul>

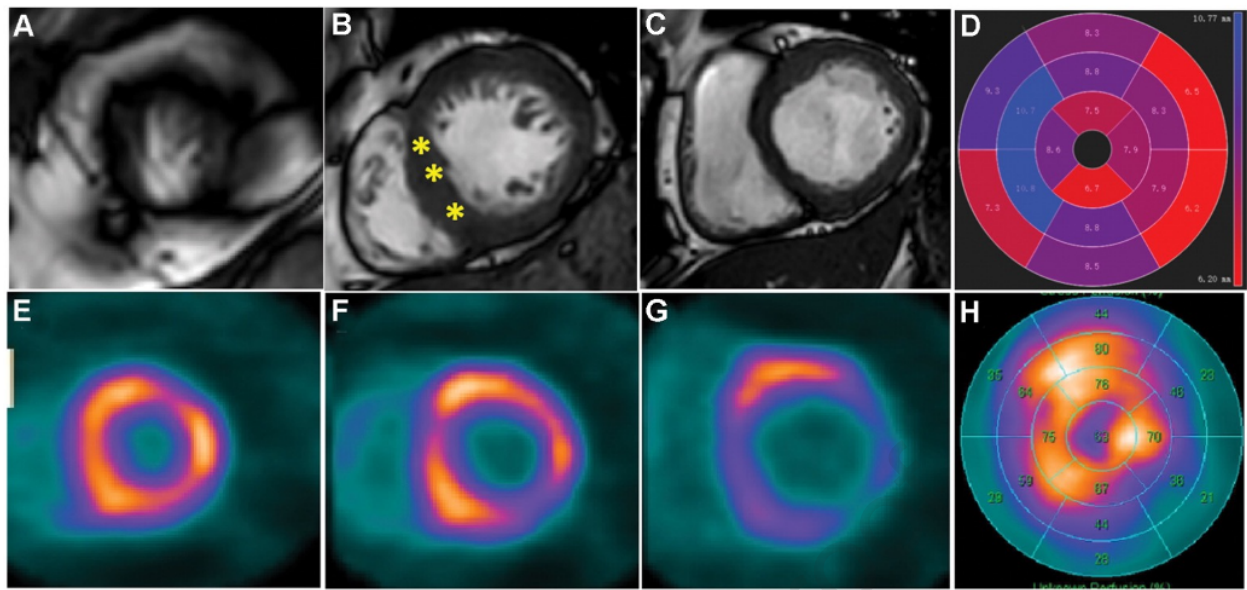
	MMP-induced ECM degradation		Pressure-overload, mice (133)	<ul style="list-style-type: none"><li>• No difference in LV mass, LVEF or collagen content</li></ul>	heart failure patients (132)	<ul style="list-style-type: none"><li>• Reduced number of cardiovascular deaths up to 180 days</li><li>• No difference in cardiac-related hospitalisations</li></ul>
--	-----------------------------	--	-------------------------------	--	------------------------------	--



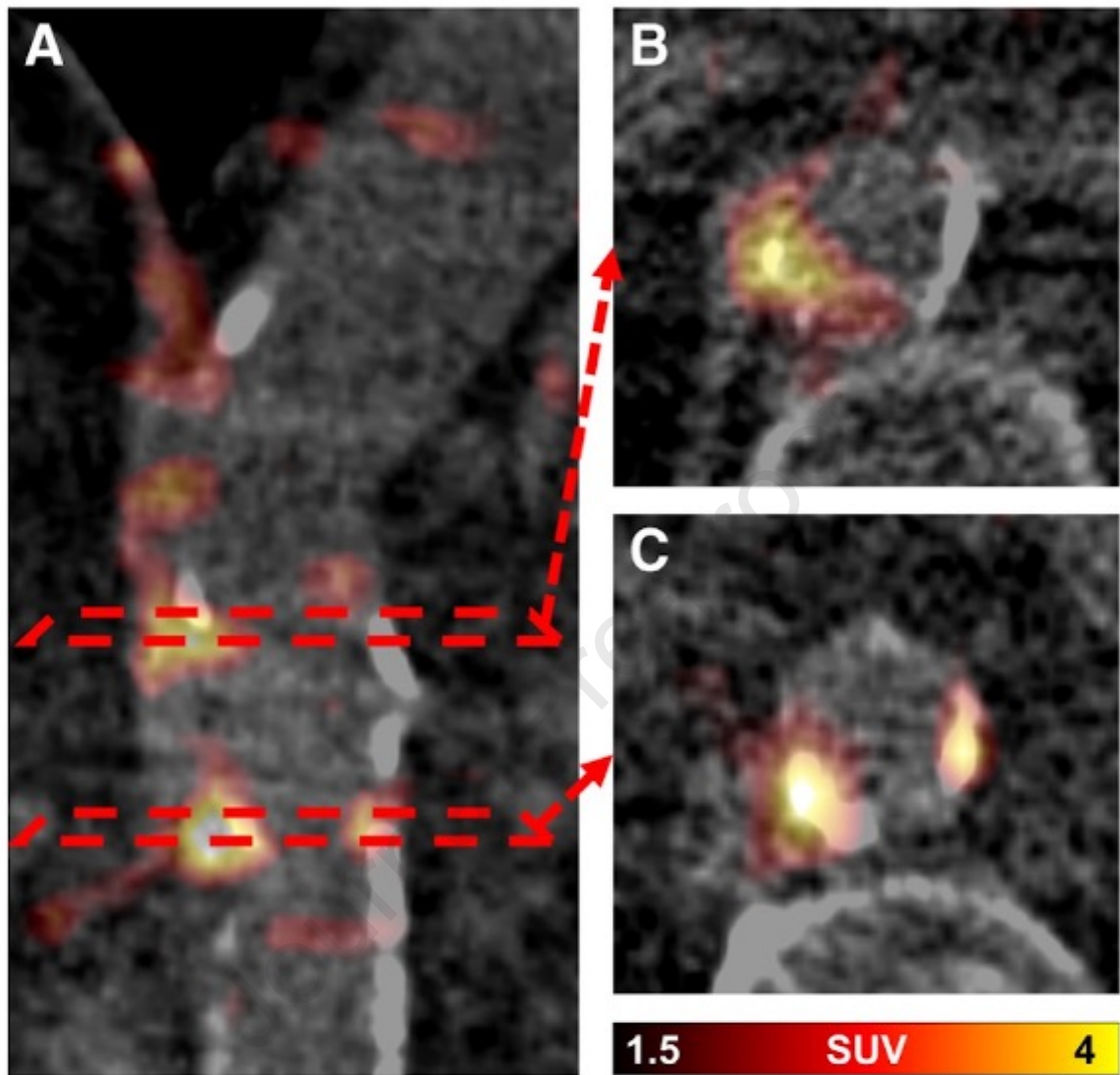


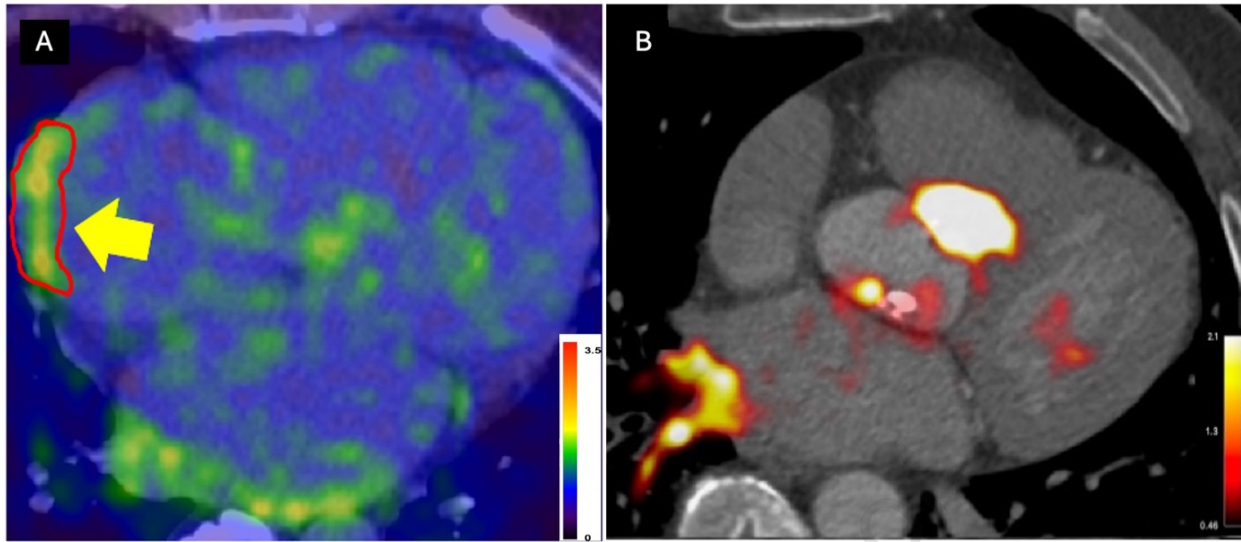


Journal Pre-proof



Journal Pre-proof





**Declaration of interests**

The authors declare that they have no known competing financial interests or personal relationships that could have appeared to influence the work reported in this paper.

The authors declare the following financial interests/personal relationships which may be considered as potential competing interests:

Paolo Anna Erba reports a relationship with SIEMENS that includes: consulting or advisory and speaking and lecture fees. Paolo Anna Erba reports a relationship with Novartis Pharmaceuticals Corporation that includes: consulting or advisory, funding grants, and speaking and lecture fees. Paolo Anna Erba reports a relationship with Springer Healthcare Limited that includes: equity or stocks. Paolo Anna Erba reports a relationship with Pfizer that includes: funding grants. Antti Saraste reports a relationship with AstraZeneca Pharmaceuticals LP that includes: consulting or advisory and speaking and lecture fees. Antti Saraste reports a relationship with Pfizer that includes: consulting or advisory and funding grants. Antti Saraste reports a relationship with Abbott that includes: speaking and lecture fees. Antti Saraste reports a relationship with Bristol Myers Squibb Co that includes: speaking and lecture fees. Antti Saraste reports a relationship with Janssen Pharmaceuticals Inc that includes: speaking and lecture fees. Jan Bucerus reports a relationship with International Atomic Energy Agency that includes: funding grants, non-financial support, and travel reimbursement. Jan Bucerus reports a relationship with European Association of Nuclear Medicine that includes: board membership. Olivier Gheysens reports a relationship with General Electric Company that includes: speaking and lecture fees. Ronny Buechel reports a relationship with General Electric Company that includes: speaking and lecture fees. Ronny Buechel reports a relationship with Pfizer Inc that includes: speaking and lecture fees. Ronny Buechel reports a relationship with Gilead Sciences Inc that includes: speaking and lecture fees. If there are other authors, they declare that they have no known competing financial interests or personal relationships that could have appeared to influence the work reported in this paper.

# 1 Cardiovascular PET imaging of fibroblast activation

## 2 *A review of the current literature*

3  
4 Krithika Loganath<sup>1</sup>, Neil Craig<sup>1</sup>, Anna Barton<sup>1</sup>, Shruti Joshi<sup>1</sup>, Constantinos Anagnostopoulos<sup>2</sup>, Paola  
5 Anna Erba<sup>3,4</sup>, Andor W.J.M. Glaudemans<sup>4</sup>, Antti Saraste<sup>5,6</sup>, Jan Bucerius<sup>7</sup>, Mark Lubberink<sup>8</sup>, Olivier  
6 Gheysens<sup>9</sup>, Ronny R. Buechel<sup>10</sup>, Gilbert Habib<sup>11,12</sup>, Oliver Gaemperli<sup>13</sup>, Alessia Gimelli<sup>14</sup>, Fabien  
7 Hyafil<sup>15,16</sup>, David E. Newby<sup>1</sup>, Riemer H.J.A Slart<sup>17,18</sup>, Marc R. Dweck<sup>1</sup>

8  
9 <sup>1</sup>BHF Centre of Cardiovascular Science, University of Edinburgh, Edinburgh, United Kingdom

10 <sup>2</sup>Clinical, Experimental Surgery & Translational Research, Biomedical Research Foundation, Academy  
11 of Athens, Athens, Greece

12 <sup>3</sup>Nuclear Medicine, Department of Translational Research and New Technology in Medicine,  
13 University of Pisa, Pisa, Italy

14 <sup>4</sup>Department of Nuclear Medicine and Molecular Imaging, Medical Imaging Center, University  
15 Medical Center Groningen, University of Groningen, Groningen, The Netherlands

16 <sup>5</sup>Turku PET Centre, Turku University Hospital and University of Turku, Kiinamyllynkatu, Turku, Finland

17 <sup>6</sup>Heart Center, Turku University Hospital, Turku, Finland

18 <sup>7</sup>Department of Nuclear Medicine, Georg-August University Göttingen, University Medicine  
19 Göttingen, Göttingen, Germany

20 <sup>8</sup>Department of Surgical Sciences/Radiology, Uppsala University, Uppsala, Sweden

21 <sup>9</sup>Department of Nuclear Medicine, Cliniques Universitaires Saint-Luc, Brussels, Belgium

22 <sup>10</sup>Department of Nuclear Medicine, Cardiac Imaging, University Hospital Zurich, Zurich, Switzerland

23 <sup>11</sup>Cardiology Department, APHM, La Timone Hospital, Marseille, France

24 <sup>12</sup>Aix Marseille Université, IRD, APHM, MEPHI, IHU-Méditerranée Infection, Marseille, France

25 <sup>13</sup>HeartClinic, Hirslanden Hospital Zurich, Hirslanden, Switzerland

26 <sup>14</sup>Fondazione Toscana G. Monasterio, Pisa, Italy

27 <sup>15</sup> Department of Nuclear Medicine, DMU IMAGINA, Georges-Pompidou European Hospital,  
28 Assistance Publique - Hôpitaux de Paris, University of Paris, Paris, France

29 <sup>16</sup>PARCC, INSERM, University of Paris, Paris, France

30 <sup>17</sup>Medical Imaging Centre, Department of Nuclear Medicine & Molecular Imaging, University of  
31 Groningen, University Medical Center Groningen, Groningen, The Netherlands

32 <sup>18</sup>Faculty of Science and Technology Biomedical, Photonic Imaging, University of Twente, Enschede,  
33 The Netherlands

34

35

36 **Abstract: 137**37 **Word count: 4499**38 **Figures: 6**39 **Tables: 4**40 **References: 134**

41

42 **Abstract**

43

44 Fibrosis is one of the key healing responses to injury, especially within the heart where it helps to  
45 maintain structural integrity following acute insults such as myocardial infarction. However, if it  
46 becomes dysregulated then fibrosis can become maladaptive leading to adverse remodelling,  
47 impaired cardiac function and heart failure. Fibroblast activation protein is exclusively expressed by  
48 activated fibroblasts, the key effector cells of fibrogenesis, and has a unique extracellular domain  
49 that is an ideal ligand for novel molecular imaging probes. Fibroblast activation protein inhibitor  
50 (FAPI) radiotracers have been developed for PET imaging, demonstrating high selectivity for  
51 activated fibroblasts across a range of different pathologies and disparate organ systems. In this  
52 review, we will summarize the role of fibroblast activation protein in cardiovascular disease and how  
53 FAPI radiotracers might improve the assessment and treatment of patients with cardiovascular  
54 diseases.

55

56

57 **Key words: Fibroblast, Fibroblast activation protein inhibitor (FAPI), Positron Emission**  
58 **Tomography, Cardiac magnetic resonance, Cardiac Computed Tomography,**

59 Introduction

60

61 **Fibrosis- friend and foe**

62

63 Fibrosis is one of the fundamental healing responses to injury and a highly conserved process across  
64 organ systems. In the short term, this process maintains tissue integrity and organ function.  
65 However, in the absence of regulation, excessive fibrosis can become harmful, leading to scarring,  
66 increased rigidity and progressive organ dysfunction (1). Indeed, myocardial fibrosis underlies almost  
67 every cardiomyopathic condition, making it a key target for imaging and therapeutic intervention.  
68 Yet the key to the success of such strategies will be targeting inappropriate and excessive fibrosis at  
69 an early stage whilst leaving the protective processes unscathed. The duality of fibrosis in the  
70 cardiovascular system is perhaps best illustrated by myocardial infarction (MI). In the acute phase,  
71 fibrosis is protective, providing structural integrity within the friable necrotic myocardium, and  
72 protecting against myocardial rupture. In contrast, later inappropriate fibrosis can lead to adverse  
73 remodelling, impaired diastolic and systolic function and the development of heart failure with the  
74 risk of fatal arrhythmias (2). An improved understanding of the timing of appropriate and  
75 inappropriate fibrotic responses after MI will be key in preventing the transition to heart failure and  
76 sudden cardiac death whilst leaving the protective scar intact.

77

78 The non-invasive identification of fibrosis is important. Current cardiovascular magnetic resonance  
79 (CMR) methods are useful in identifying established fibrosis. In particular, T1 mapping techniques  
80 can identify reversible and diffuse interstitial fibrosis using native T1 values and extracellular volume  
81 percentage (ECV%). Late gadolinium enhancement (LGE) techniques can identify irreversible  
82 replacement fibrosis. These approaches are widely employed in clinical practice to aid the diagnosis  
83 and risk stratification of patients with various cardiac conditions but are limited to documenting  
84 established fibrosis in the myocardium without the spatial resolution to assess fibrosis in the valves  
85 and atherosclerotic plaques in vascular structures (3). Furthermore, they do not identify whether  
86 fibrogenesis remains active in the heart, being unable to distinguish between active and inactive or  
87 burnt-out disease: is it scarred or is it scarring (4)? Novel molecular positron emission tomography  
88 (PET) radiotracers, such as radiolabelled fibroblast activation protein inhibitors (FAPI), can address  
89 these shortcomings by identifying activated fibroblasts and active fibrosis, with the benefit of  
90 tracking fibroblast activity over time and in response to treatment (5, 6). FAPI imaging is now  
91 being widely used to investigate fibroblast activation and fibrosis activity across organ systems,  
92 building upon the success of these tracers in imaging cancer-associated fibroblasts (7).

93

94 The Inflammatory, Infective, Infiltrative, and Innervation (4Is) Committee is a collaboration between  
95 the European Association of Cardiovascular Imaging (EACVI) and the European Association of  
96 Nuclear Medicine (EANM). Members of this committee identified FAPI PET imaging as one of the  
97 most promising new areas of molecular cardiovascular imaging and felt that the imaging community  
98 should be introduced to this novel application. Our aim is, therefore, to summarize the current  
99 status of this field as well as to outline what we consider to be the most exciting areas for future  
100 research with this novel imaging technique. This review will explore the imaging of cardiovascular  
101 fibrosis activity with FAPI PET. We will briefly discuss the pathophysiology of various cardiovascular

102 conditions, the role of activated fibroblasts in these and how FAPI is useful in targeting these  
103 processes. We will then review the existing FAPI literature in myocardial disease, before finally  
104 describing how this exciting area may develop in the future and improve both our understanding of  
105 cardiovascular fibrosis and in guiding patient care.

106

## 107 **Fibrosis and Activated Fibroblasts**

108

### 109 *Myocardium*

110

111 Cardiac fibrosis is a result of interstitial expansion from excess extracellular matrix (ECM) deposition  
112 within the myocardium, predominantly composed of fibrillar collagens. Cross-linking of these fibers  
113 reduces myocardial elasticity and contractile capacity, leading to diastolic and systolic dysfunction.  
114 Cardiac fibrosis is categorized into two forms, though overlap appears. Replacement fibrosis is  
115 irreversible scarring from intense myocardial injury and myocyte necrosis, such as MI or acute  
116 myocarditis. In contrast, diffuse interstitial fibrosis is reversible and associated with chronic disease  
117 processes like aortic stenosis and hypertension. Left unchecked, it can progress to replacement  
118 fibrosis (8).

119

### 120 *Atherosclerosis*

121 Atherosclerotic plaques form from low-density lipoprotein deposits in vessel walls. Immune cell  
122 infiltration triggers smooth muscle proliferation, forming early 'fatty streaks'. (9) These evolve into  
123 fibrous plaques, causing luminal narrowing and creating sites for clot formation. Beneath the fibrous  
124 cap, cell apoptosis and cholesterol crystals form a necrotic core. (10, 11).

125

### 126 *Activated fibroblasts*

127 Fibroblasts are a group of cells in the connective tissue that synthesize collagen and other  
128 components of the extracellular matrix (ECM). They predominantly arise from epicardial cells that  
129 have undergone epithelial to mesenchymal transformation (EMT) (12, 13), but can also arise from  
130 endothelial cells within the interventricular septum (14), neural crest cells in the right atrium (15),  
131 adventitial fibroblasts (16) and local smooth muscle cell-to-fibroblast transition (17). In their  
132 quiescent form, fibroblasts are tasked with the role of maintaining tissue homeostasis, constantly  
133 monitoring the myocardium through its cycles of contraction and relaxation, and replenishing the  
134 ECM as required (18).

135

136 Activated fibroblasts are the key cells driving fibrogenesis in the myocardium and other organs of  
137 the body. In the myocardium they exist in two forms. They are first activated into an intermediate  
138 form called proto-myofibroblasts, which acquire proliferative and migratory properties, enabling  
139 them to move into areas of damage, secreting predominantly type I and type III collagens and cross-  
140 linking the ECM to generate wound healing (19). Further autocrine signalling and the action of  
141 fibroblast modulators (e.g extra domain A fibronectin and hyaluronan) result in the maturation of

142 proto-myofibroblasts into myofibroblasts. Myofibroblasts provide enhanced contractile strength  
143 with the aid of  $\alpha$ -smooth muscle actin ( $\alpha$ -SMA) stress fibres, which form stable adherence plaques  
144 between cell membranes and the ECM junction (20, 21) (Figure 1). In addition, activated fibroblasts  
145 have a key role in matrix remodelling, secreting matrix metalloproteinases (MMPs), which degrade  
146 components of the extracellular matrix, as well as their tissue inhibitors (TIMPs). The balance  
147 between collagen production and the activity of MMPs and TIMPs influences the nature and  
148 composition of the extracellular matrix. In atherosclerosis, metalloproteinase production by  
149 activated fibroblasts can weaken the fibrous cap overlying the necrotic core, predisposing it to  
150 rupture and myocardial infarction.

151

## 152 **Fibroblast Activation Protein**

153 Fibroblast activation protein (FAP) is a 760-amino acid transmembrane surface glycoprotein that is  
154 expressed almost exclusively on activated fibroblasts. It has a role in normal developmental  
155 processes during embryogenesis and organ formation but is not expressed by quiescent fibroblasts.  
156 FAP was first discovered in 1994 (22) and has both dipeptidyl transferase (DPP) and endopeptidase  
157 activity (23), the latter readily differentiating it from the more ubiquitous DPP IV receptors (CD26).  
158 The specificity of FAP for activated fibroblasts makes it a good marker of these cells and, therefore, of  
159 fibrosis activity (24). Indeed, fibroblasts expressing FAP have been identified in a range of conditions  
160 across different organ systems, including wound healing, liver, and lung fibrosis (25, 26). FAP is also a  
161 key protein in cancer-associated fibroblasts, where its protease activity is associated with cell  
162 migration and a poor prognosis explaining the strong interest in this molecular target in oncology  
163 (27).

164

165

## 166 **Fibroblast Activation Protein Inhibitor Radiotracers**

167 Quinoline-based FAP-specific inhibitors (28) bound to a DOTA chelator and then to a radioisotope:  
168 either gallium-68 ( $^{68}\text{Ga}$ ) or aluminium fluoride-18 ( $^{18}\text{F}$ -AlF) have been developed (29). FAPI-02 and  
169 FAPI-04 were clinically promising initial radiotracers, demonstrating good stability in human serum, a  
170 strong affinity and high specificity for FAP+ cells, and high target-to-background ratio (TBR).  
171 However, hepatobiliary excretion was high, affecting image quality (29-31). This improved with the  
172 development of FAPI-46. Fluorinated tracers have the benefit of larger yields, lower radiation  
173 dosage and longer half-lives but they are incompatible with DOTA. As such, the smaller NOTA  
174 molecule is used for  $^{18}\text{F}$ -AlF binding, resulting in the development of FAPI-74. ONCOFAP is an ultra-  
175 high affinity FAP ligand with superior specificity for FAP+ cells and excellent target-to-background  
176 ratios. It can be attached to NOTA and DOTA molecules to bind reliably to  $^{68}\text{Ga}$ ,  $^{18}\text{F}$ -AlF and even  
177 the larger  $^{177}\text{Lu}$  for theranostic use (32, 33) (Table 1).

178

## 179 Advantages of FAPI tracers

180 FAPI tracers target the more exclusive endopeptidase activity of fibroblast activation protein, making  
181 them highly specific for this protein (34). Moreover, after binding FAP, FAPI becomes rapidly and  
182 almost completely internalised into FAP+ fibroblasts with minimal release into surrounding tissues

183 (34). These properties suggest excellent tracer specificity, and consistent with this, very little non-  
184 specific background uptake is observed when FAPI tracers are injected in vivo.

185

186 In oncology, FAPI tracers have demonstrated improved signal-to-noise in many solid organ tumours  
187 compared to  $^{18}\text{F}$ -fluorodeoxyglucose ( $^{18}\text{F}$ -FDG) (35, 36). Increasing evidence is now demonstrating the  
188 value of FAPI PET imaging in detecting non-malignant fibrosis activity across organ systems, including  
189 the detection of lung, liver, and kidney fibrosis as well as systemic pro-fibrotic conditions (37-40).

190 Histological validation of the FAPI PET signal has been widely performed across an array of different  
191 conditions, demonstrating the co-localization and correlation of FAPI PET activity with FAP+  
192 fibroblasts on immunohistochemistry. Blocking studies have confirmed that this uptake is specific to  
193 the FAP protein (41-45).

194

195 FAPI tracers demonstrate favourable pharmacokinetics with rapid renal clearance and reduced  
196 hepatobiliary excretion. Both the  $^{68}\text{Ga}$  and  $^{18}\text{F}$ -AIF-FAPI tracers have short half-lives (68 and 109  
197 mins, respectively) and their administration is associated with low radiation doses (both  $<2$  mSv per  
198 100 MBq administered). Another benefit of FAPI radiotracers is their fast uptake time and blood  
199 clearance, resulting in good contrast to noise ratios as early as 10 minutes following injection,  
200 although optimal cardiovascular image quality appears to occur at 60 minutes (34, 46, 47). In  
201 addition, minimal uptake is seen in healthy myocardium with  $\text{SUV}_{\text{mean}}$  values ranging from 0.35 to 1.2  
202 (29, 48, 49). The shorter positron range of fluoride tracers offers the benefit of improved image  
203 resolution (50). Finally, unlike  $^{18}\text{F}$ -FDG imaging, FAPI PET does not require any dietary modification  
204 prior to imaging.

205

#### 206 Disadvantages of FAPI tracers

207 Certain FAPI radioligands demonstrate hepatobiliary excretion resulting in uptake within the liver  
208 (29). In addition, moderate physiologic uptake is seen in the pancreas (51) and kidneys (52) with the  
209 highest physiologic uptake seen in the uterus (53) making it difficult to discern true pathological  
210 FAPI uptake in these and adjacent structures. With the current evidence, it remains uncertain as to  
211 which exact subpopulation of activated fibroblasts these FAPI radiotracers bind to.

212

213 Perhaps the main disadvantages of FAPI tracers relate to their availability and expense. FAPI is a new  
214 radiotracer that is not yet widely available commercially although the advent of fully automated  
215 processes will help achieve standardization (33, 54). Standard gallium generators can only provide 1  
216 to 3 patient doses per production resulting in high per-dose production costs (55). Fluorinated  
217 alternatives such as  $^{18}\text{F}$ -AIF-FAPI overcome this hurdle with a cyclotron able to generate more doses  
218 (32). More importantly, the feasibility and cost of FAPI imaging are likely to improve with its more  
219 widespread use. Indeed, the exciting preliminary results from FAPI imaging in cancer suggest that it  
220 may well replace a reasonable proportion of the  $^{18}\text{F}$ -FDG PET imaging in future clinical practice (35).  
221 When one considers that more than 1 million  $^{18}\text{F}$ -FDG PET scans are performed annually in the US  
222 alone, this is likely to drive wider availability and lower costs of FAPI tracers for use across various  
223 disease states.

224

## 225 **FAPI Imaging in Cardiovascular Disease**

226 The nascent literature supporting the role of FAPI radiotracers in cardiovascular disease is expanding  
227 (56). The first published report of a 67-year-old man with pancreatic ductal adenocarcinoma, a  
228 history of ischaemic heart disease, and a reduced left ventricular ejection fraction of 41%. Intense  
229  $^{68}\text{Ga}$ -FAPI uptake was noticed in his left ventricular (LV) myocardium in addition to his known  
230 tumour and metastases (57). It was hypothesized that cardiotoxicity following chemotherapy may  
231 have contributed to his cardiac dysfunction and intense FAPI uptake. Subsequently, in 185 oncology  
232 patients who had undergone  $^{68}\text{Ga}$ -FAPI PET/CT imaging of their underlying cancer, increased focal  
233 FAPI uptake was identified in the myocardium of 42 patients. There was a positive correlation  
234 between this myocardial  $^{68}\text{Ga}$ -FAPI uptake and cardiovascular risk factors, a history of MI, type 2  
235 diabetes mellitus as well as the prior use of platinum-based chemotherapy agents and radiotherapy  
236 (58). Amongst a subgroup with concomitant echocardiography,  $^{68}\text{Ga}$ -FAPI uptake was higher in  
237 patients with reduced compared to normal LVEF.

238

## 239 Myocardial Infarction

240 In small animal models, FAPI uptake occurs in areas of infarction peaking at day 6 after MI with  
241 higher uptake in the border regions and minimal uptake in the remote myocardium up to 35 days.  
242 These spatio-temporal patterns of uptake confirmed that  $^{68}\text{Ga}$ -FAPI-PET provides different  
243 information to the detection of established myocardial fibrosis and scarring with CMR. Areas of  
244 uptake corresponded with autoradiography and immunofluorescence staining for FAP + fibroblasts  
245 (59, 60)(Figure 2).

246

247 Clinical studies similarly demonstrated good concordance between FAPI uptake and infarcted  
248 myocardium. In a study of 35 people up to 11 days post myocardial infarction, the volume of  
249 fibroblast activation protein uptake positively correlated with LGE on CMR and exceeded the area of  
250 perfusion defect on myocardial perfusion scanning. Indeed, 14% of segments demonstrating FAPI  
251 uptake exhibited no LGE and normal T1 and T2 levels. The volume of FAPI uptake correlated with a  
252 fall in LVEF at a median of 140 days post myocardial infarction in 14 of the 35 patients (61). Similar  
253 results were seen in smaller studies where FAPI uptake extended beyond the infarct zone (62, 63)  
254 and correlated with late LV remodelling (64) and LVEF (62, 65) (Table 2). PET-MR benefits from  
255 combining both LGE-based fibrosis imaging with FAPI uptake. Initial studies have demonstrated that  
256 FAPI volumes correlate with LGE and serum biomarkers (64, 66), with more research underway  
257 (ClinicalTrials.gov Identifier: NCT04723953). Aside from PET imaging,  $^{99\text{m}}\text{Tc}$ -labeled fibroblast  
258 activation protein inhibitor ( $^{99\text{m}}\text{Tc}$ -HFAPi) SPECT imaging has similarly demonstrated increased FAP  
259 activity in patients post acute MI which exceed perfusion defects and inversely correlated with LVEF  
260 (67).

261

## 262 Myocardial diseases

263 Myocardial FAPI uptake has been investigated in a variety of cardiomyopathies and conditions that  
264 can lead to heart failure (Table 3). In animal models, FAPI uptake is increased in pressure-overload  
265 conditions, heart failure with reduced ejection fraction (HFrEF), heart failure with preserved ejection  
266 fraction (HFpEF) (68-70) and anthracycline-induced cardiotoxicity (71). Similar results have been

267 found in clinical studies with increased LV myocardial FAPI uptake across a range of  
268 cardiomyopathies (69, 70, 72-77)

269

270 Interestingly, FAPI uptake did not necessarily correspond to areas of reduced perfusion on  $^{13}\text{N-NH}_3$   
271 imaging in non-ischaemic cardiomyopathy (70) (Figure 3) or with established scarring in LGE in  
272 chronic thromboembolic pulmonary hypertension (76) and hypertrophic cardiomyopathy (73). FAPI  
273 uptake did, however, correlate positively with the 5-year sudden cardiac death score in  
274 hypertrophic cardiomyopathy, demonstrating a potential prognostic role in this group (73) (Figure  
275 4).

276

277 Myocardial FAPI uptake is increased in patients with severe aortic stenosis about to undergo  
278 transcatheter aortic valve implantation. FAPI volume correlates with markers of heart failure such as  
279 N-terminal pro b-type natriuretic peptide (NT-proBNP) and left ventricular ejection fraction,  
280 indicating a potential for its use in prognostication. As with other cardiovascular conditions, FAPI  
281 uptake did not necessarily correspond to areas of fibrosis identified on CMR (78). Studies are  
282 currently in progress to investigate these further (ClinicalTrials.gov Identifier: NCT06047561). (Figure  
283 5)

284

285 Finally, numerous case reports have now described increased myocardial  $^{68}\text{Ga}$ -FAPI uptake across a  
286 range of cardiovascular conditions, including anthracycline-induced cardiotoxicity (57), hypertensive  
287 heart disease (79), cardiac sarcoidosis (80) and Fabry's disease (81). Trials are ongoing at the  
288 moment investigating further cardiomyopathies (ClinicalTrials.gov Identifier: NCT04555642,  
289 NCT05756608).

290

291

## 292 Atherosclerosis

293 Activated fibroblasts have been implicated across the spectrum of atherosclerosis, from initial  
294 plaque formation in response to injury and MMP production to constrictive vascular remodelling  
295 and the formation of stable plaques as the cycle of inflammation and injury perpetuates (82, 83).  
296 Two retrospective studies in oncology and IgG4-related disease populations have assessed FAPI  
297 imaging in vivo. FAPI uptake was seen in only about half of calcified arterial lesions (Figure 5) (84),  
298 with the intensity of FAPI uptake correlating inversely with the extent of calcification (85). An  
299 elevated body mass index was the only individual cardiovascular risk factor that significantly  
300 correlated with FAPI uptake, although Wu and colleagues found that the presence of 4 or more risk  
301 factors positively correlated with the number of FAPI + lesions and  $\text{TBR}_{\text{mean}}$  (85), indicating that FAPI  
302 imaging may be useful in high-risk populations. These were non-cardiac gated scans and both groups  
303 reported significant noise and partial-volume effects, so prospective data with dedicated vascular  
304 scanning protocols would be warranted to investigate this further. No study has yet reported FAPI  
305 imaging in the coronary arteries.

306

## 307 Inflammatory vascular diseases

308 Vascular uptake has been demonstrated in patients with Takayasu's arteritis, giant cell arteritis and  
309 IgG4-related disease (35, 86, 87). A case report of a patient with Takayasu's arteritis reported that  
310  $^{68}\text{Ga}$ -FAPI uptake was detected in the thickened thoraco-abdominal aortic wall as well as in the  
311 carotid and subclavian arteries where  $^{18}\text{F}$ -FDG uptake was absent (86).  $^{68}\text{Ga}$ -FAPI uptake has also  
312 been documented in IgG4-related disease, with potentially increased sensitivity in organs (pancreas  
313 and bile duct) compared to  $^{18}\text{F}$ -FDG (38, 87).

314

### 315 Arrhythmia

316 Atrial fibrillation is the commonest sustained arrhythmia and is associated with changes in atrial  
317 structure and atrial fibrosis (88, 89). Increased  $^{18}\text{F}$ -AIF-FAPI uptake was seen in the atria of beagle-  
318 models of AF which corresponded to autoradiography and FAP + fibroblasts on histology, with  
319 similar results seen in patients with AF (90) (Figure 6). Focal  $^{68}\text{Ga}$ -FAPI uptake is commonly seen  
320 following pulmonary vein isolation, especially following cryoballoon ablation (91). As with other  
321 conditions, further studies are warranted to investigate the role of activated fibroblast in the  
322 pathology of AF and atrial cardiomyopathy as well as its recurrence following pulmonary vein  
323 isolation.

324

### 325 **Other fibrosis radiotracers**

326

327 Other fibrosis radiotracers are currently being investigated with promising results.  $^{18}\text{F}$ -Fluciclatide  
328 binds to the  $\alpha_v\beta_3$  integrin transmembrane receptor responsible for ECM production and  
329 angiogenesis with increased tracer activity observed in acutely infarcted myocardium that  
330 demonstrated a positive correlation with improved subsequent myocardial recovery (92). Proline is a  
331 pre-cursor of collagen, which gets incorporated into developing collagen and might therefore serve  
332 as a marker of fibrosis formation (93). However, the presence of various isomeric forms, each with  
333 its different radiotracer properties, makes standardisation and manufacture a challenge. Thus far,  
334 fluorinated proline ( $^{18}\text{F}$ -Proline) has had mixed results in extra-cardiac preclinical and clinical studies  
335 (94, 95).

336

### 337 **The future of FAPI radiotracers**

338

339 Whilst activated fibroblast imaging in cardiovascular disease has a promising future, it remains in its  
340 infancy. Considerable work is required before we can fully appreciate how this technique may aid  
341 our understanding of activated fibroblasts and fibrosis activity in cardiovascular disease, let alone  
342 appreciate whether it might fulfil a useful clinical role. Based upon the information currently  
343 available from both cardiovascular and non-cardiovascular diseases, we believe it is helpful to  
344 speculate about how the field may evolve, to outline what we consider the most exciting areas for  
345 research, and to discuss potential future applications of FAPI-PET in patients with cardiovascular  
346 disease. We hope that this will stimulate discussion and ideas for future studies in this field.

347

### 348 Detection of early disease

349 Molecular PET imaging provides unrivalled sensitivity in the detection of disease and can potentially  
350 detect the activity of disease processes before they are apparent with other modalities. An excellent  
351 example is  $^{18}\text{F}$ -NaF PET, which can detect calcification activity before calcium is evident on CT (96).  
352 FAPI PET might provide similar sensitivity for myocardial fibrosis allowing the detection of activated  
353 fibroblasts prior to the deposition of collagen and ECM – the changes detectable on CMR. This may  
354 prove of particular value in patients with chemotherapy-induced cardiotoxicity, where the early  
355 identification of myocardial injury could help guide the use and dose of chemotherapy regimens and  
356 the need for cardioprotective medication, especially as its utility in cancer care continues to expand.  
357 Other potential clinical uses related to early detection include the prompt identification of left  
358 ventricular decompensation in patients with aortic stenosis and the differentiation of  
359 cardiomyopathy from athlete's heart. Importantly, not all FAP+ fibroblasts will result in fibrosis, as  
360 seen in studies of acute MI patients where areas of FAPI uptake extend beyond that of LGE, even at  
361 follow-up (61). Investigation of how FAP+ fibroblasts behave with disease progression and how they  
362 can be modulated to avoid fibrosis, warrants further exploration but suggests that FAPI imaging  
363 might identify a reversible stage of the disease.

364

#### 365 Detecting fibrosis in thin-walled structures

366

367 The high sensitivity of FAPI PET can be used to identify fibroblast activation in thin-walled structures  
368 where reliable fibrosis imaging has previously been challenging, particularly in the right ventricle and  
369 cardiac atria. Detection of right ventricular fibroblast activity might be of particular value in patients  
370 with arrhythmogenic cardiomyopathy, pulmonary hypertension, and congenital heart disease. The  
371 role that fibrosis plays in these conditions might be elucidated, and patient diagnosis, risk  
372 stratification, and difficult management decisions might be aided by such techniques (58, 76, 77).  
373 Similarly, with the atria, FAPI PET holds promise in improving our understanding of atrial  
374 cardiomyopathy and the triggers to atrial fibrillation. We know that atrial fibrosis is implicated in the  
375 development of atrial fibrillation and is positively linked to the development of atrial thrombus and  
376 subsequent stroke risk (97-99) but have previously not been able to image it reliably. Indeed,  
377 detection of atrial LGE with CMR remains a challenge and is limited to a handful of expert centres.

378

379 In larger arterial vessels such as the aorta and femoral arteries, FAPI has been useful to characterise  
380 plaques with thin fibrous caps that may be prone to rupture compared to their stable calcific  
381 equivalent (84, 85). Smaller calibre vessels such the carotids and coronary arteries have not yet been  
382 investigated although the ability to identify at-risk plaques would be useful to target primary and  
383 secondary prevention therapy in these patients. As with established CMR methods, partial volume  
384 issues are a concern and further research is required to optimise PET imaging in these thin walled  
385 structures.

386

#### 387 Active versus established disease

388

389 Molecular imaging is already used clinically to differentiate active from inactive or burnt-out disease  
390 states and to guide therapy. A good example is cardiac sarcoidosis, where  $^{18}\text{F}$ -FDG is used to identify

391 ongoing myocardial inflammation, providing complementary information to CMR, that is used to  
392 guide the need for immunosuppressive agents (100). Given the central pathological role of fibrosis,  
393 FAPI PET might fulfil a similar role across a wide range of cardiomyopathic processes and is likely to  
394 lead to important insights into the spatiotemporal activation of fibroblasts in different  
395 cardiovascular conditions. For the evaluation of systemic diseases such as atherosclerosis, vasculitis,  
396 sarcoidosis and amyloidosis, total body PET may prove of additional value. Dynamic quantification  
397 with whole-body coverage allows assessment of disease activity across the body and can provide  
398 optimal quantification while evaluating cross-over interactions between different organs and tissue  
399 in the same subject (101, 102).

400

401 Important questions regarding fibroblast activation can be addressed for the first time in humans.  
402 For example, when does fibroblast activity start and stop following MI? Is it the same in larger versus  
403 smaller infarcts and the same in the infarct zone versus the remote myocardium? Once the normal  
404 pattern of fibrosis activity has been established following a particular insult, then FAPI PET may help  
405 to differentiate protective forms of fibrosis from maladaptive patterns. This would allow us to  
406 identify the patients most likely to benefit from the raft of novel anti-fibrotic medication currently  
407 under development (Table 4) (103, 104).

408

#### 409 Predicting disease progression and monitoring response to treatment

410

411 Promising initial data suggest that FAPI PET can track changes in fibroblast activation in response to  
412 antifibrotic treatments in systemic sclerosis-related interstitial lung disease and IgG4 -related disease  
413 (38, 105). An exciting possibility is that FAPI PET could be used similarly in patients with  
414 cardiovascular disease to identify with an adverse pattern of fibroblast activation who can then be  
415 targeted with therapies at a potentially reversible stage of their disease process. FAPI PET could then  
416 be used to confirm treatment response and to identify patients in need of more aggressive  
417 management strategies. In addition, FAPI PET could then be considered to assess long-term  
418 treatment response to such therapies and to identify the time point at which such therapies could  
419 be stopped. This would allow a truly personalized approach to the treatment of cardiovascular  
420 disease and direct the right treatment to the right patient at the right time.

421

422 FAPI PET might also prove of value in accelerating the development of novel anti-fibrotic therapies.  
423 The pervasiveness of fibrosis across various disease processes underlines the urgent need to develop  
424 such treatment. Whilst some existing antifibrotic therapies have been shown to be effective in non-  
425 malignant diseases such as interstitial pulmonary fibrosis (106, 107) these frequently come at the  
426 cost of side effects such as nausea, vomiting and photosensitivity. Alternative strategies are  
427 therefore required. FAPI imaging might prove a useful tool in enriching study populations with  
428 patients that have a reversible disease state in whom benefit might be most likely to develop.  
429 Moreover, FAPI PET could then be used to track response to therapy as a marker of efficacy. Such  
430 changes in fibroblast activation could be detected earlier and with greater sensitivity utilising this  
431 technique, compared to existing approaches which have to wait until overt changes in myocardial  
432 fibrosis burden or systolic function become apparent (Table 4). In that way FAPI PET might  
433 accelerate and reduce the cost of phase 2 clinical trials.

434

435

436

**437 FAP as a therapeutic marker and target**

438 There is considerable interest in FAP+ cells as a therapeutic target. Whilst genetic deletion of FAP  
439 does not greatly affect cardiac fibrosis, targeting of FAP+ fibroblasts holds substantial potential. CAR-  
440 T cell therapy has resulted in major advances in the treatment of cancer over recent years. Cytotoxic  
441 T cells are engineered to target cancer cells and eliminate them with little collateral damage.  
442 Recently, several preclinical studies have investigated CAR-T cell therapy targeting FAP+ fibroblasts.  
443 Lee and colleagues demonstrated promising results in a rodent model of mesothelioma and used  
444 <sup>18</sup>F-AIF-FAPI to track this treatment response (45). In a mouse model of heart failure, CAR-T cell  
445 therapy targeting FAP+ fibroblasts reduced cardiac fibrosis and led to improvements in LV systolic  
446 and diastolic function (108) with more work ongoing to ensure that this is a feasible and safe  
447 treatment in cardiovascular conditions (109, 110)

448

449 Beyond CAR-T cell therapy, an alternative approach is to modify FAPI radiotracers so that they  
450 become theranostic agents. This can be accomplished by binding the tracers to a therapeutic  
451 radioligand (e.g. <sup>131</sup>I or <sup>177</sup>Lu) that emits high-energy beta or alpha particles, which subsequently kill  
452 nearby cells. This form of therapy provides temporal control so that FAP+ fibroblasts can be targeted  
453 only at those time points when they are inappropriately activated and not indefinitely (111).  
454 Theranostic FAPI approaches have been explored in several oncological research studies (43, 112,  
455 113), but its use in cardiovascular diseases has not been investigated.

456

457

**458 Conclusion**

459 FAPI-PET is a novel molecular imaging technique that, for the first time, allows the assessment of  
460 fibroblast activation and fibrosis activity in patients with cardiovascular disease. Whilst in its infancy,  
461 initial reports are highly promising, and this approach looks set to dramatically improve our  
462 understanding of fibrosis activity across a wide range of cardiovascular disease states with important  
463 potential to accelerate novel therapeutic strategies and improve patient assessment and outcomes.

## Figures

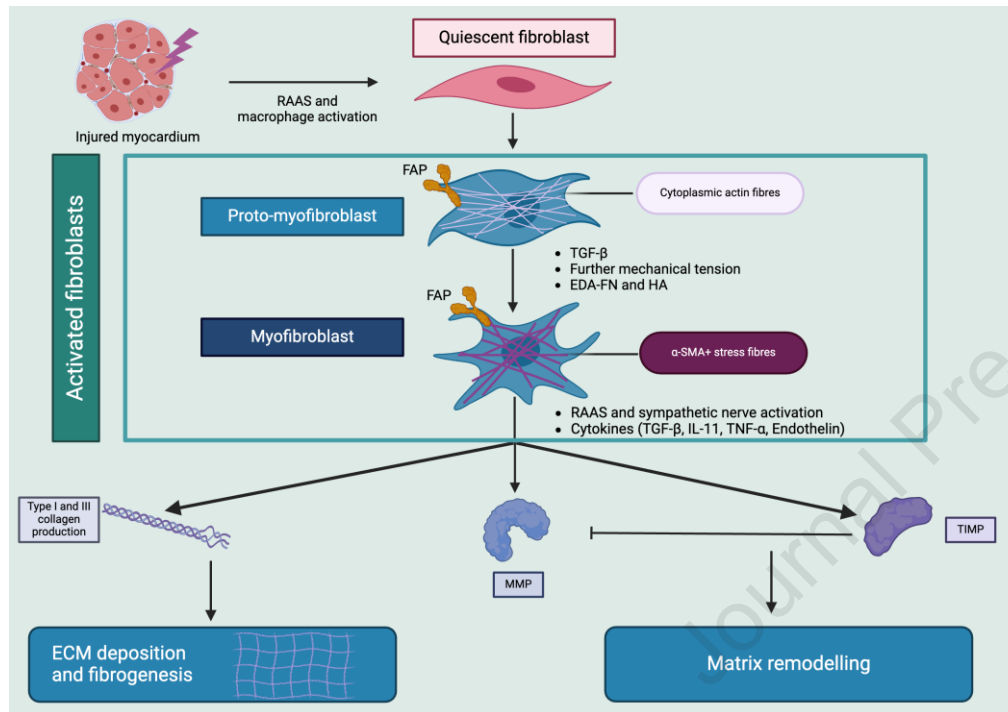


Figure 1: Cascade of myocardial fibrosis formation regulated by activated fibroblasts.

Following myocardial injury, RAAS and macrophage activation prompt the activation of the quiescent fibroblast to the intermediate proto-myofibroblast which rearranges membrane-associated actin into cytoplasmic filamentous actin fibres that form adhesion sites at membrane–ECM junctions. Further cytokine activity and synthesis of modulators that maintain the myofibroblast such as EDA-FN and HA result in maturation of the proto-myofibroblast into the myofibroblast. Myofibroblasts are characterised by the presence of thick, interconnected actin fibres that are  $\alpha$ -SMA positive and result in the formation of mature, stable adhesion plaques at membrane-ECM junctions and, hence, increased contractile strength.

RAAS: Renin-angiotensin-aldosterone- system; TGF-  $\beta$ : Transforming growth factor- Beta; IL-11: Interleukin-11; TNF- $\alpha$ : Tumour Necrosis Factor- $\alpha$ ; ECM: Extracellular matrix; MMP: Matrix metalloproteinases; TIMP: Tissue inhibitor of matrix metalloproteinases;  $\alpha$ - SMA: Alpha smooth muscle actin; HA: Hyaluronan; EDA-FN : extra domain A fibronectin

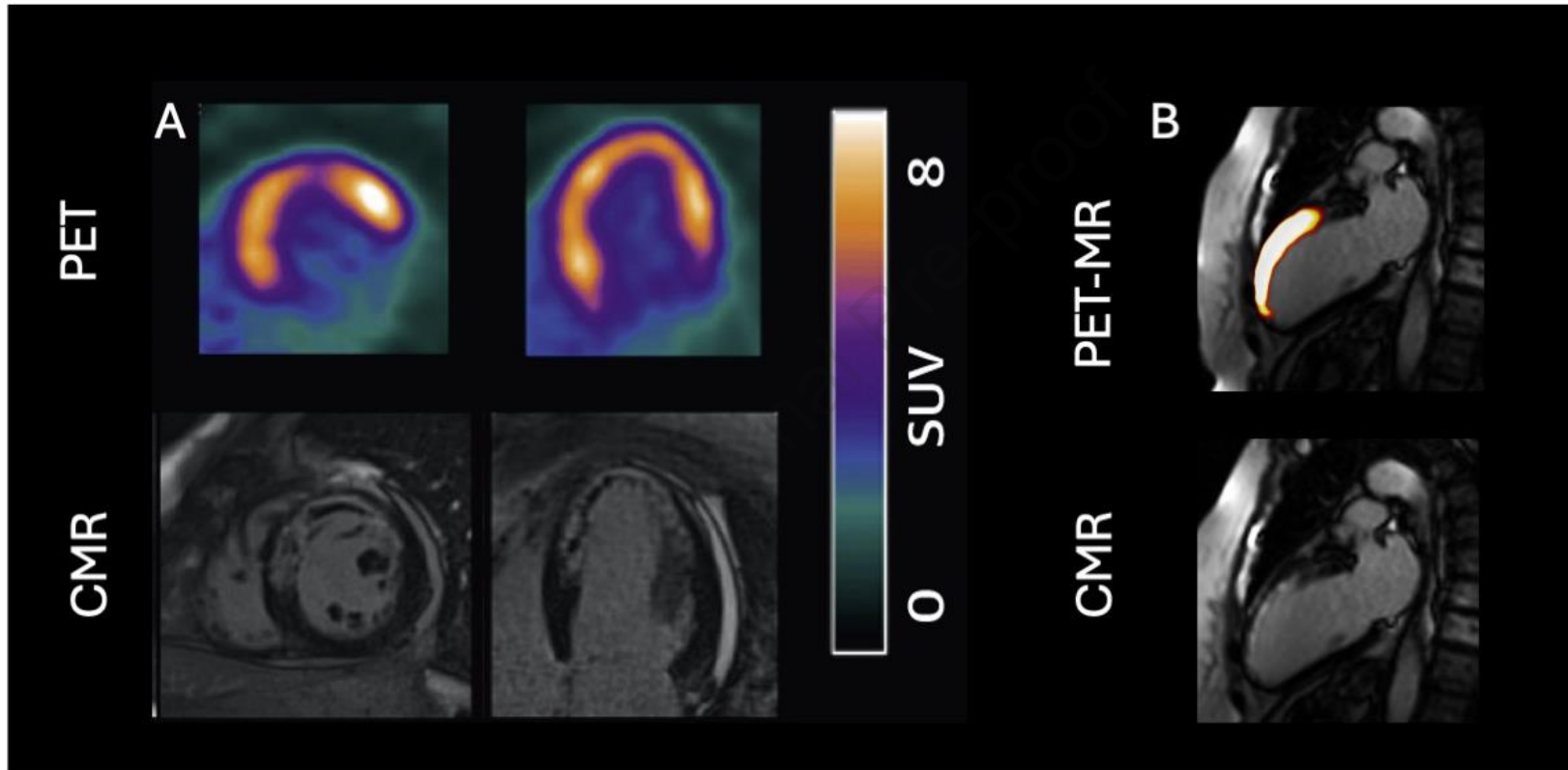


Figure 2: Examples of  $^{68}\text{Ga}$ -FAPI uptake in acute myocardial infarction

A: An example of  $^{68}\text{Ga}$ -FAPI uptake in a patient with an anterior acute myocardial infarction (top) with corresponding contrast-enhanced CMR images (bottom). This image was adapted from research published in *JNM*. Diekmann et.al. Cardiac Fibroblast Activation in Patients Early After Acute Myocardial Infarction: Integration with MR Tissue Characterization and Subsequent Functional Outcome. *J Nucl Med*. 2022. 63 (9) 1415-1423. © SNMMI.

B: Example of  $^{68}\text{Ga}$ -FAPI uptake on hybrid PET-MR (Top) using FusionQuant software (Cedars- Sinai, Los Angeles) which provides automated motion correction and smooth image processing that reduces background noise.

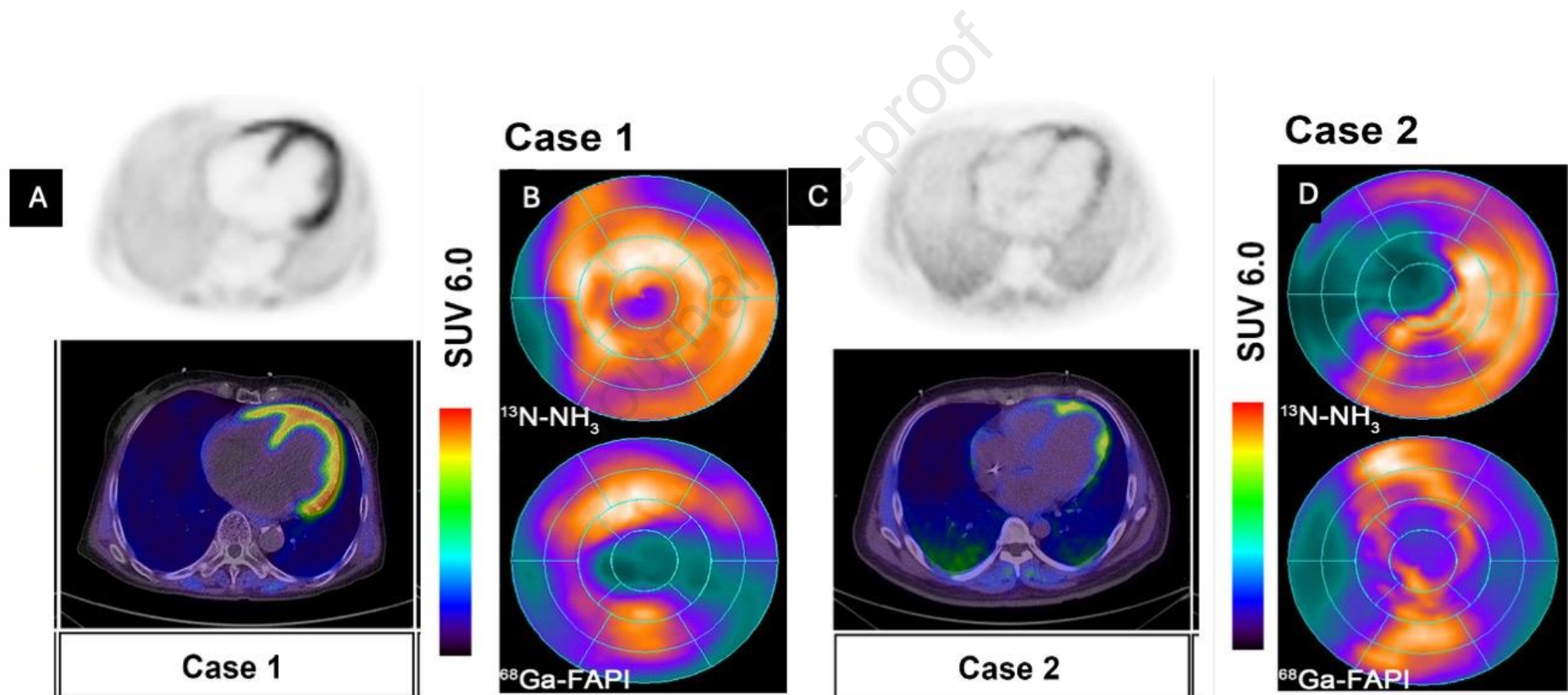


Figure 3: Examples of  $^{68}\text{Ga}$ -FAPI PET-CT uptake in patients with heart failure and reduced ejection fraction compared to polar maps of  $^{13}\text{N}$ - $\text{NH}_3$  perfusion scanning showing little correlation in patterns between the two.

A: axial view of  $^{68}\text{Ga}$ -FAPI uptake in a patient with dilated cardiomyopathy. B (top) myocardial perfusion scanning demonstrating heterogenous reduction in perfusion while  $^{68}\text{Ga}$ -FAPI (bottom) uptake shows more anterior and inferior fibroblast activation

C: Axial view of  $^{68}\text{Ga}$ -FAPI uptake in a patient with severe left ventricular systolic dysfunction and a history of ischaemic heart disease. D (top) shows a large perfusion defect in the septum while  $^{68}\text{Ga}$ -FAPI (bottom) demonstrated fibroblast activation in the anterior and inferior walls.

Adapted from research originally published in EJNMMI. Song et.al.  $^{68}\text{Ga}$ -FAPI PET visualize heart failure: from mechanism to clinic. *Eur J Nucl Med Mol Imaging*. 2023. 50 (2), 475–485 .© Springer Nature.

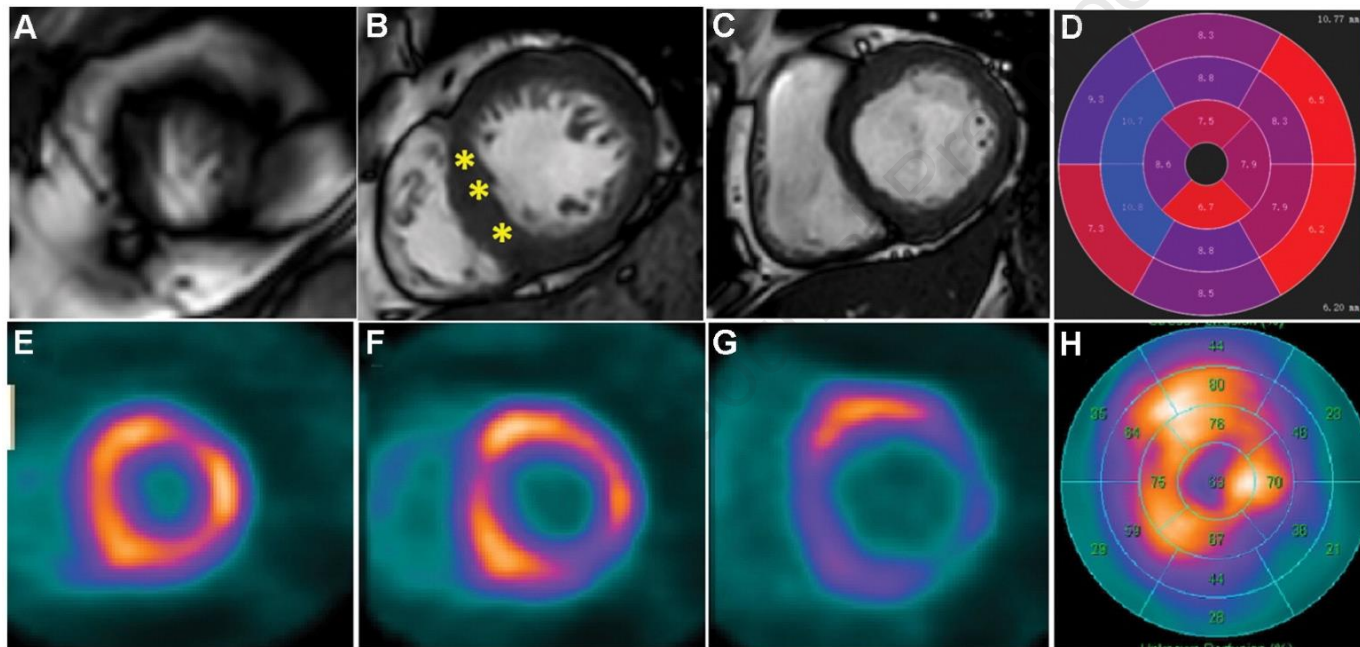


Figure 4: Example of  $^{68}\text{Ga}$ -FAPI uptake in hypertrophic cardiomyopathy

(A–D): Image of a patient with HCM demonstrating that involved myocardium extended beyond areas of hypertrophy. The selected short-axis images from cardiac MRI (A–C) showed hypertrophic midseptum (15 mm, \*), which is presented with a polar plot (D).

E–H : corresponding short-axis images of  $^{18}\text{F}$ -FAPI (E–G) and polar plot (H) indicated the larger area of cardiac fibroblast activation beyond the hypertrophic region.

This research was originally published in *Radiology*. Wang et.al. Myocardial Activity at  $^{18}\text{F}$ -FAPI PET/CT and Risk for Sudden Cardiac Death in Hypertrophic Cardiomyopathy. *Radiology*. 2022. 11;306(2):e221052.© RSNA.

Journal Pre-proof

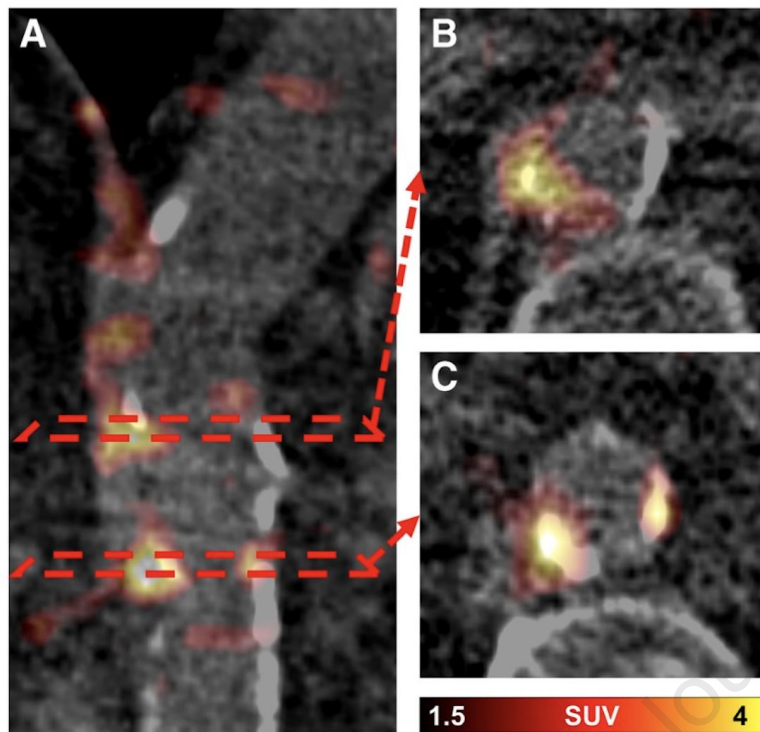


Figure 5: Example of atherosclerotic plaque FAPI uptake. This research was originally published in *EJNMMI*. Kosmala et.al. Molecular imaging of arterial fibroblast activation protein: association with calcified plaque burden and cardiovascular risk factors *Eur J Nucl Med Mol Imaging*. 2023. 50(10); 3011-3021(84).

Fused  $^{68}\text{Ga}$ -FAPI PET CT images of a patient with aortic valve atherosclerosis

A: Coronal PET-CT image demonstrating 2 major foci of  $^{68}\text{Ga}$ -FAPI uptake with corresponding axial images (B and C).

B:  $^{68}\text{Ga}$ -FAPI uptake exceeds the vessel wall calcification while a further calcified lesion shows no uptake.

C:  $^{68}\text{Ga}$ -FAPI uptake co-localized well with vessel wall calcifications

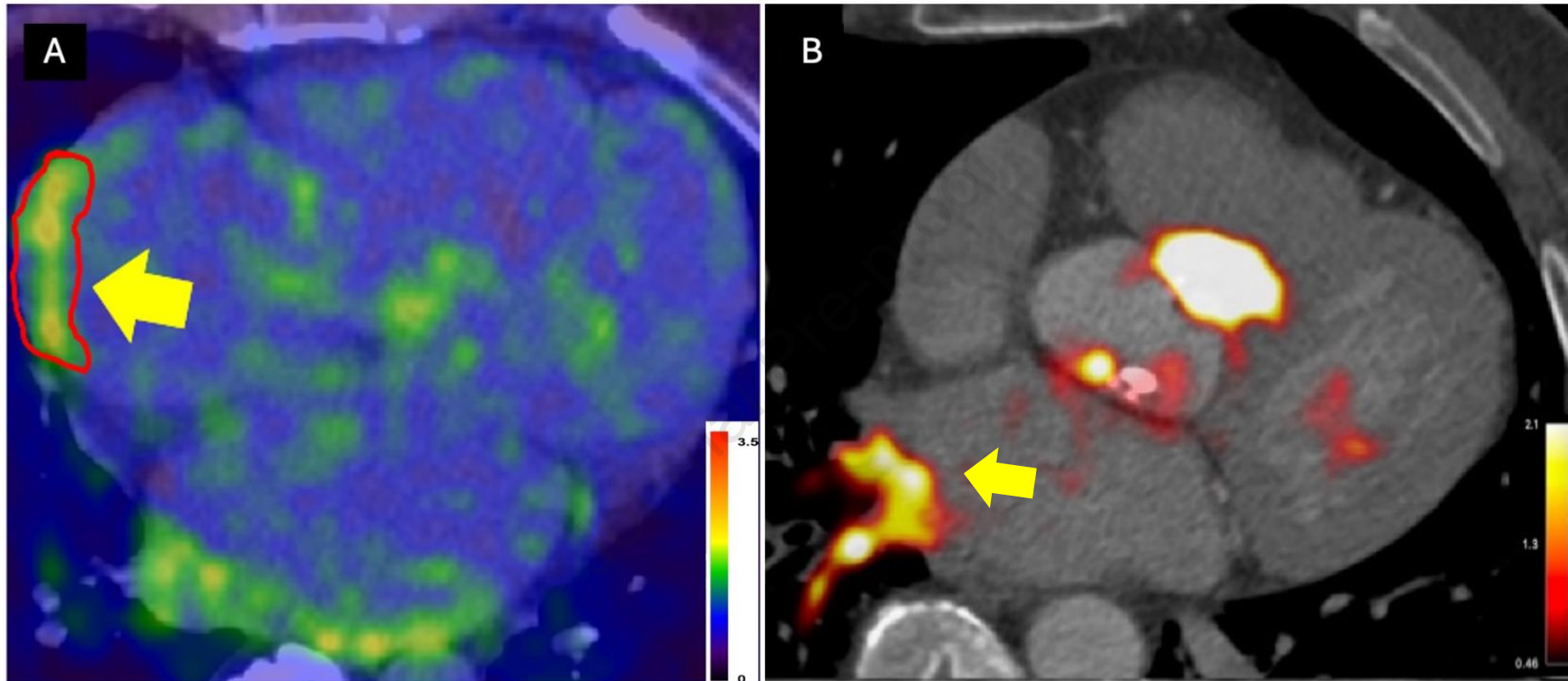
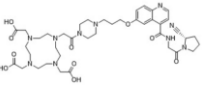


Figure 6: FAPI uptake in atrial fibrillation

A: An example of increased  $^{18}\text{F}$ -AIF-FAPI uptake in the right atrial wall (TBRmax 2.5) in a fused PET-CT . Adapted from research originally published in *JNC*. Li et.al. Li, Lina, et al. Fibroblast activation protein imaging in atrial fibrillation: a proof-of-concept study. *J. Nucl. Cardiol.* 2023. 30(6); 2712-2720(90) $^{68}\text{Ga}$ -FAPI uptake at the ostium of the left inferior pulmonary vein (A) and posterior wall of the left atrium (B) in a patient who also demonstrates  $^{68}\text{Ga}$ -FAPI in their stenotic aortic valve.

## Tables

Name	Chelator	Healthy myocardial uptake and internalisation	Hepatobiliary excretion	Tissue retention
FAPI-02  Loktev et al, 2018 (34)	DOTA	Medium	High	Low

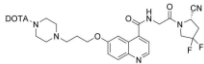
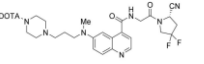
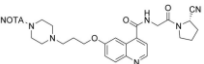
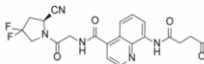
<p>FAPI-04</p>  <p>Lindner et al, 2018 (29)</p>	DOTA	Medium	Medium	Medium
<p>FAPI-46</p>  <p>Loktev et al, 2019 (48) Meyer et al, 2020 (49)</p>	DOTA	Medium	Medium	High
<p>FAPI-74</p>  <p>Giesel et al, 2021 (32) Lindner et al, 2021 (114)</p>	NOTA	High	Low	High
<p>ONCOFAP</p>  <p>Millul et al, 2021 (115) Backhaus et al, 2022 (116)</p>	NOTA and DOTA	Low	Low	High

Table 1: Properties of various FAPI radioligands based on dosimetry and biodistribution data across various organs.

Healthy myocardial uptake: SUVmeans at 1 hour post injection range from 0.32 to 1.2

Hepatobiliary excretion: SUVmeans at 1 hour post injection range from 0.5 – 1.6

Tissue retention: measured by the percentage drop in SUVmean in tumours in 3 hours post injection, ranging from 12-75%

Table 2: Key studies investigating FAPI imaging in Myocardial Infarction

<b>Myocardial infarction</b>				
<b><i>Preclinical studies</i></b>				
<b>Title</b>	<b>Model</b>	<b>Tracer</b>	<b>Imaging modality</b>	<b>Key results</b>
Varasteh et al (59)	Murine	<sup>68</sup> Ga-FAPI	PET-CT, autoradiography	<ul style="list-style-type: none"> <li>• Peak radiotracer uptake observed at 6 days post MI with return to baseline by 14 days</li> <li>• Peri-infarct regions demonstrated more intense uptake than infarct regions</li> <li>• No remote myocardial uptake up to 14 days</li> <li>• FAP expression confirmed in areas on <sup>68</sup>Ga-FAPI uptake on immunofluorescence</li> <li>• FAP+ cells were observed 3 and 8 times more in the border zones than in infarct and remote myocardium, respectively</li> </ul>
Qiao et al, 2022 (60)	Rat	<sup>68</sup> Ga-FAPI	PET-CT, Autoradiography, Immunofluorescenc, H&E staining	<ul style="list-style-type: none"> <li>• Peak radiotracer uptake in infarcted myocardium with gradual decline until day 35, where uptake was similar to the sham-operated group</li> <li>• No significant remote <sup>68</sup>Ga-FAPI uptake was noted up to 35 days</li> </ul>

				<ul style="list-style-type: none"> <li>Higher uptake demonstrated at the border zones on autoradiography</li> </ul>	
<b><u>Clinical studies</u></b>					
<b>Title</b>	<b>Cohort and design</b>	<b>Tracer</b>	<b>Imaging modality</b>	<b>Key points</b>	<b>Correlation with imaging and serum biomarkers</b>
Diekmann et al (61)	35 STEMI patients, prospective	<sup>68</sup> Ga-FAPI	PET-CT, SPECT, CMR	<ul style="list-style-type: none"> <li>Volume of <sup>68</sup>Ga-FAPI uptake correlated with a fall in LVEF at 140 days post infarct in 14 of the 35 patients</li> <li>Segmental SUV<sub>mean</sub> inversely correlated with CMR wall thickening</li> </ul>	<ul style="list-style-type: none"> <li><sup>68</sup>Ga-FAPI uptake areas exceeded areas of fibrosis as identified by LGE, T1 and T2 levels</li> <li>Positive correlation observed between <sup>68</sup>Ga-FAPI volume and maximum serum creatine kinase and C-reactive protein</li> </ul>
Diekmann et al (63)	12 STEMI patients, Prospective	<sup>68</sup> Ga-FAPI	PET-CT, SPECT, CMR	<ul style="list-style-type: none"> <li>Significant <sup>68</sup>Ga-FAPI uptake in the infarct, extending into the peri-infarct zones</li> </ul>	<ul style="list-style-type: none"> <li><sup>68</sup>Ga-FAPI uptake areas exceeds infarct areas identified on SPECT and CMR LGE imaging</li> </ul>
Kessler et al (65)	5 STEMI and 5 NSTEMI patients, Prospective	<sup>68</sup> Ga-FAPI	PET-CT	<ul style="list-style-type: none"> <li>All patients had significant <sup>68</sup>Ga-FAPI uptake in the myocardium</li> <li>A complete to partial concordance was observed of visual <sup>68</sup>Ga-FAPI myocardial uptake and areas supplied by the culprit vessel</li> </ul>	<ul style="list-style-type: none"> <li><sup>68</sup>Ga-FAPI uptake volume was positively correlated with peak CK level and negatively correlated with LVEF</li> </ul>

Xie et al (62)	14 STEMI patients and 14 healthy volunteers, Prospective	<sup>68</sup> Ga-FAPI	PET-CT and CMR	14 patients post STEMI <ul style="list-style-type: none"> <li>Significant <sup>68</sup>Ga-FAPI uptake was observed over infarct zones and beyond</li> <li>Baseline TBR<sub>max</sub> inversely correlated with LV function at 7 weeks</li> </ul>	<ul style="list-style-type: none"> <li>Areas of <sup>68</sup>Ga-FAPI uptake extended beyond LGE on CMR</li> </ul>
Zhang et al (64)	26 STEMI patients, Prospective	<sup>68</sup> Ga-FAPI	PET-MR	<ul style="list-style-type: none"> <li>Increased <sup>68</sup>Ga-FAPI volumes and TBR<sub>max</sub> at baseline correlated with reduced LVEF at 1 year</li> <li>Patients who had late LV remodelling ( increase in LVESV &gt;10% from baseline) had a higher baseline <sup>68</sup>Ga-FAPI volume</li> </ul>	<ul style="list-style-type: none"> <li>No significant correlation between <sup>68</sup>Ga-FAPI volumes and serum biomarkers such as NT-proBNP and serum troponin I.</li> <li>Baseline <sup>68</sup>Ga-FAPI predicted late LV remodelling better than LGE% and LGE volume on CMR</li> </ul>
Kupusovic et al (66)	4 NSTEMI and 7 STEMI patients, prospective	<sup>68</sup> Ga-FAPI	PET-MR	<ul style="list-style-type: none"> <li>Higher <sup>68</sup>Ga-FAPI SUV<sub>max</sub> was observed in STEMI than NSTEMI patients although not statistically significant</li> </ul>	<ul style="list-style-type: none"> <li>Mean <sup>68</sup>Ga-FAPI uptake volume exceeded estimated MRI infarct size but showed a strong positive correlation</li> <li><sup>68</sup>Ga-FAPI uptake volume had a strong correlation with LDH and peak creatine kinase</li> </ul>

PET: Positron Emission Tomography; CT: Computed Tomography; <sup>68</sup>Ga-FAPI: Gallium-labelled fibroblast activation protein inhibitor; MI: Myocardial infarction; FAP: Fibroblast activation protein; H&E: hematoxylin and eosin; STEMI: ST-elevation myocardial infarction; NSTEMI: Non ST-elevation myocardial infarction; CK: Creatine kinase; SPECT: Single-photon emission computed tomography; CMR: Cardiac magnetic resonance imaging; LGE: Late gadolinium enhancement; TBR<sub>max</sub>: Maximum tissue-to-background ratio; LV: Left ventricle; LVEF: Left ventricular ejection fraction; NT-proBNP: N-terminal pro b-type natriuretic peptide

Table 3: Key studies of FAPI imaging in cardiomyopathies

<b>Myocardial diseases</b>					
<b><i>Preclinical studies</i></b>					
<b>Title</b>	<b>Condition</b>	<b>Model</b>	<b>Tracer</b>	<b>Imaging Modality</b>	<b>Key points</b>
Wang et al (68)	Pressure-overload	Rat	<sup>68</sup> Ga-FAPI	PET-CT, PET-MR, Echocardiography, Immunohistochemistry	<ul style="list-style-type: none"> <li>• Areas of increased <sup>68</sup>Ga-FAPI uptake corresponded with areas of myocardial hypertrophy on CMR</li> <li>• Early <sup>68</sup>Ga-FAPI uptake at 4 weeks corresponded to a reduced LVEF at 8 weeks</li> <li>• Increased myocardial <sup>68</sup>Ga-FAPI uptake in areas corresponding FAP expression on immunohistochemistry</li> </ul>
Sun et al (69)	HFrEF	Rat	<sup>18</sup> F-AIF-FAPI	PET-CT, Immunohistochemistry, Masson staining	<ul style="list-style-type: none"> <li>• Increased <sup>18</sup>F-AIF-FAPI uptake in the LV myocardium in rats corresponded to post-mortem areas of FAP+ cells and interstitial and vascular fibrosis</li> </ul>
Song et al (70)	HFrEF	Murine	<sup>68</sup> Ga-FAPI	PET-CT	<ul style="list-style-type: none"> <li>• A positive correlation was seen between baseline LV myocardial <sup>68</sup>Ga-FAPI uptake and decline in LV contractility and increased LV dilatation at 28 days</li> </ul>

Wei et al (71)	Anthracycline-induced cardiotoxicity	Rat	<sup>68</sup> Ga-FAPI	PET-CT, Echocardiography, Immunohistochemistry, Masson staining	<ul style="list-style-type: none"> <li><sup>68</sup>Ga-FAPI uptake was significantly higher in rats with cardiotoxicity compared to control rats at weeks 3 and 6 although no significant change in LVEF was seen between groups</li> <li>Enalapril treatment for 3 weeks reduced the intensity of <sup>68</sup>Ga-FAPI uptake, preserved LVEF and reduced myocardial fibrosis on Masson staining</li> </ul>	
<b><i>Clinical studies</i></b>						
<b>Title</b>	<b>Condition</b>	<b>Cohort and design</b>	<b>Tracer</b>	<b>Imaging Modality</b>	<b>Key points</b>	<b>Correlation with imaging and serum biomarkers</b>
Wang et al (74)	Multiple non- ischaemic cardiomyopathies	29 patients, Prospective	<sup>68</sup> Ga-FAPI	PET-CT, echocardiography	<ul style="list-style-type: none"> <li>22 of the 29 scanned patients had heterogenous LV myocardial FAPI uptake</li> <li>10 patients had RV myocardial FAPI uptake across a spectrum of aetiologies</li> </ul>	<ul style="list-style-type: none"> <li>SUV<sub>max</sub> correlated significantly with LVEDD on echocardiography</li> </ul>
Song et al (70)	HFrEF	7 patients , 20 participants without cardiac disease, Prospective	<sup>68</sup> Ga-FAPI	PET-CT, <sup>13</sup> N-NH <sub>3</sub> perfusion scan	<ul style="list-style-type: none"> <li>Significantly elevated LV myocardial <sup>68</sup>Ga-FAPI uptake was seen in patients compared to healthy volunteers</li> </ul>	<ul style="list-style-type: none"> <li>Areas of <sup>68</sup>Ga-FAPI uptake did not correspond with areas of reduced perfusion on <sup>13</sup>N- NH<sub>3</sub> myocardial perfusion scan</li> </ul>

Wang et al (73)	HCM	50 patients with HCM vs 20 healthy volunteers, Prospective	<sup>18</sup> F-AIF-FAPI	PET-CT, CMR (without gadolinium)	<ul style="list-style-type: none"> <li>• Significantly higher LV myocardial <sup>18</sup>F-AIF-FAPI uptake in patients compared to healthy volunteers</li> <li>• 32 (64%) patients had increased <sup>18</sup>F-AIF-FAPI uptake in the RV myocardium and 4 (8%) had significant <sup>18</sup>F-AIF-FAPI uptake in the atria, 3 of whom had AF.</li> <li>• Increased <sup>18</sup>F-AIF-FAPI uptake positively correlated with the 5-year sudden cardiac death score and risk of malignant arrhythmia</li> </ul>	<ul style="list-style-type: none"> <li>• Increased <sup>18</sup>F-AIF-FAPI uptake was seen in all hypertrophied segments but also in non-hypertrophied segments in 84% of patients</li> <li>• <sup>18</sup>F-AIF-FAPI had a positive relationship with NT-proBNP and hs-cTnI and negative relationship with LVEF</li> </ul>
Chen et al (76)	Chronic thromboembolic pulmonary hypertension	13 patients with CTEPH, prospectively recruited	<sup>68</sup> Ga-FAPI	PET-CT, CMR, RHC	<ul style="list-style-type: none"> <li>• 10 of the 13 patients demonstrated significant free RV wall <sup>68</sup>Ga-FAPI uptake</li> <li>• <sup>68</sup>Ga-FAPI uptake positively correlated with RV wall thickness and negatively correlated with RVEF</li> </ul>	<ul style="list-style-type: none"> <li>• Only 27% of significant RV <sup>68</sup>Ga-FAPI uptake corresponded to LGE on CMR</li> <li>• No correlation between <sup>68</sup>Ga-FAPI uptake and pulmonary haemodynamic parameters on RHC</li> </ul>

Gu et al (77)	Pulmonary arterial hypertension	16 patients with PAH, prospectively recruited	<sup>68</sup> Ga-FAPI	PET-CT, echocardiography, RHC	<ul style="list-style-type: none"> <li>12 of the 16 patients had significant RV free wall and insertion point <sup>68</sup>Ga-FAPI uptake</li> </ul>	<ul style="list-style-type: none"> <li><sup>68</sup>Ga-FAPI uptake correlated with TAPSE on echocardiography</li> <li>No significant correlation between <sup>68</sup>Ga-FAPI uptake and pulmonary haemodynamic parameters on RHC</li> </ul>
Finke et al (75)	Checkpoint-inhibitor (ICI) associated myocarditis	26 patients who received ICI, 3 with myocarditis, Retrospective analysis	<sup>68</sup> Ga-FAPI	PET-CT, CMR	<ul style="list-style-type: none"> <li><sup>68</sup>Ga-FAPI uptake significantly higher in ICI myocarditis patients</li> </ul>	<ul style="list-style-type: none"> <li>2/3 patients with ICI had MRI. 1 had globally elevated T1-mapping and another had basal LGE. T2 mapping was normal</li> </ul>
Wang et al (72)	Cardiac AL-amyloidosis	30 patients with AL amyloidosis (27 with cardiac involvement and 3 without), Prospective	<sup>68</sup> Ga-FAPI	PET-CT, CMR, Echocardiography	<ul style="list-style-type: none"> <li>80% of AL CA patients had increased intensity of myocardial <sup>68</sup>Ga-FAPI uptake</li> </ul>	<ul style="list-style-type: none"> <li>4 patients with LGE on CMR also had significant <sup>68</sup>Ga-FAPI uptake</li> <li>FAPI uptake correlated with Mayo stage and NTpro-BNP levels, ECV percentage on CMR and negatively correlated with LVPW thickness and LVEF on CMR</li> </ul>

PET-CT: Positron Emission Tomography and Computed Tomography; PET-MR: Positron Emission Tomography and Magnetic Resonance imaging; HFpEF: Heart Failure with preserved Ejection Fraction; HFrEF: Heart Failure with reduced Ejection Fraction; CMR: Cardiac Magnetic Resonance; <sup>68</sup>Ga-FAPI: Gallium-labelled fibroblast activation protein inhibitor; <sup>18</sup>F-AIF- FAPI: Aluminium fluoride- labelled fibroblast activation protein inhibitor; FAP: Fibroblast activation protein; LV: Left ventricle; LVEF: Left ventricular ejection fraction; DCM: Dilated Cardiomyopathy; HCM: Hypertrophic cardiomyopathy; SUV<sub>max</sub>: Maximum Standardised Uptake Value; SUV<sub>mean</sub>: Mean Standardised Uptake Value SPECT: Single-photon emission computed tomography; LGE: Late gadolinium enhancement; LVEDD: Left Ventricular End Diastolic Diameter; TBR<sub>max</sub>: Maximum tissue-to-background ratio; NT-proBNP: N-terminal pro b-type natriuretic peptide; <sup>13</sup>N- NH<sub>3</sub>: <sup>13</sup>N- ammonia; LVOT: Left ventricular outflow tract; RV: Right ventricle; hs-cTnI: High-sensitivity cardiac troponin I; RHC: Right heart catheterization; RVEF: Right ventricular ejection fraction; ICI: Checkpoint-inhibitor; CTEPH: Chronic Thromboembolic pulmonary hypertension; PAH: Pulmonary Arterial Hypertension; TAPSE: Tricuspid annular plane systolic excursion; AL- amyloidosis: Light-chain amyloidosis; ECV: Extracellular volume; LVPW: Left ventricle posterior wall

Table 4: Novel anti-fibrotic medications under development

Receptor	Function	Name of drug	Preclinical data		Clinical data	
			Cohort and model	Key points	Cohort and design	Key points
CTGF Also known as CCN2	Mediates ECM production in pathological states	CTGF-mAb	Pressure-overload, mice(117)	<ul style="list-style-type: none"> <li>Improved LV systolic function</li> <li>Reduced cardiomyocyte hypertrophy in murine models</li> </ul>	Nil	
			DCM, mice (118)	<ul style="list-style-type: none"> <li>Improved LV systolic and diastolic dysfunction</li> </ul>	Nil	
			MI, mice (119)	<ul style="list-style-type: none"> <li>Improved 7-day survival</li> <li>Improved LV function</li> </ul>	Nil	

				<ul style="list-style-type: none"> <li>No difference in infarct size or 7 week survival</li> </ul>		
Galectin-3	Interacts with aldosterone to promote macrophage infiltration and mediates cardiac fibroblast proliferation	Modified Citrus Protein (MCP)	HF, rats (120)	<ul style="list-style-type: none"> <li>Improved LV function</li> <li>Reduced expression of collagen 1 and 3 genes</li> </ul>	Nil	
			HF, mice (121)	<ul style="list-style-type: none"> <li>Improved LV function</li> <li>Reduction in cardiac hypertrophy and fibrosis when treated in combination with an aldosterone antagonist</li> </ul>		
MicroRNA- 132-3p (miR-132)	Downregulates expression of Forkhead box O3 (FOXO3) which is anti-hypertrophic and suppresses calcium handling and myocardial contractility	Anti-miR-132	Post-MI HFrEF, mice (122)	<ul style="list-style-type: none"> <li>Improved LVEF and NT pro-BNP levels</li> <li>Reduction in myocardial interstitial fibrosis on in mice</li> </ul>	Prospective randomised, double-blind, placebo-controlled trial of 28 patients with HFrEF (LVEF 30-49%) (123)	<ul style="list-style-type: none"> <li>No adverse reactions</li> <li>Combined endpoint of NT pro-BNP reduction of &gt;10% and LVEF increase of &gt;2% was achieved in 79% in the pharmacodynamically active group vs 46% in the inactive group</li> </ul>
Renin	Inhibits angiotensin II and promotes angiotensin II-	Aliskiren	Pressure-overload, mice (124)	<ul style="list-style-type: none"> <li>Improved LVEF, LVFS and collagen volume</li> </ul>	Nil	

	independent reduction in TGFB-1 and collagen production					
TGF- $\beta$	Inhibition of TGF- $\beta$ reduces collagen deposition in the extracellular matrix	Pirfenidone	Pressure-overload, mice (125)		PIROUTTE trial-randomised, double-blind, placebo-controlled trial in 47 HFpEF patients (126)	<ul style="list-style-type: none"> <li>• Reduction of ECV and LV mass on CMR</li> <li>• 26% of treated patients has side effects ( nausea, insomnia, rash) although similar to placebo group</li> </ul>
			MI (127)	<ul style="list-style-type: none"> <li>• Lower total LV fibrosis</li> <li>• Higher LVEF</li> </ul>		
Phosphorylated Smad2 inhibitor	Phosphorylated Smad2, a downstream product of TGF-beta, increases ECM production	FT011	MI, rat (128)	<ul style="list-style-type: none"> <li>• Improved LVEF</li> <li>• Reduced amount of cardiac fibrosis in non-infarct regions</li> </ul>	Nil	
Matrix metalloproteinase (MMP) inhibitors	MMPs promote the degradation of ECM and adverse	PG-116800	Pressure-overload, mice (129)	<ul style="list-style-type: none"> <li>• Lower LVEDV and intersitial fibrosis in MMP knockout (KO) mice</li> <li>• No difference in LVEF (129)</li> </ul>	Randomised placebo-controlled double-blind trial of 253 post-	<ul style="list-style-type: none"> <li>• No difference in mortality, cardiac admissions or LVEF</li> <li>• Higher incidence of gastrointestinal</li> </ul>

	myocardial remodelling		MI, mice (131)	<ul style="list-style-type: none"> <li>• MMP-29 KO mice had a lower 7-day survival mostly due to cardiac rupture.</li> <li>• LVESD and LVEDD were higher in KO mice than WT, while collagen I and III were lower in KO mice (131)</li> </ul>	STEMI HFrEF patients (130)	disturbance and joint stiffness in the treatment group
Relaxin	Stimulates fibroblast differentiation and collagen deposition as well as promoting MMP-induced ECM degradation	Seralaxin	MI, mice (132)	<ul style="list-style-type: none"> <li>• Lower LVEDP</li> <li>• Reduced collagen volume in infarct and border regions</li> <li>• No significant difference in LVEF</li> </ul>	RELAX-AHF trial- a randomised placebo-controlled trial of Seralaxin in 1161 acute heart failure patients (133)	<ul style="list-style-type: none"> <li>• Improved patient-reported dyspnoea but no difference in days alive out of hospital up to 60 days</li> <li>• Reduced number of cardiovascular deaths up to 180 days</li> <li>• No difference in cardiac-related hospitalisations</li> </ul>
			Pressure-overload, mice (134)	<ul style="list-style-type: none"> <li>• No difference in LV mass, LVEF or collagen content</li> </ul>		

CTGF: Connective tissue growth factor; ECM: Extracellular matrix; CTGF-mAb: Connective tissue growth factor- monoclonal antibody; LV: Left ventricle; MI: Myocardial infarction; DCM: Dilated cardiomyopathy; MCP: Modified citrus protein; HF: Heart failure; miR-132: MicroRNA- 132-3p; LVEF: Left ventricular ejection fraction; NT pro-BNP: N-terminal prohormone of brain natriuretic peptide; HFrEF: Heart failure with reduced ejection fraction; PD: Pharmacodynamically; LVFS: Left ventricular fractional shortening; ECV: Extracellular volume; CMR: Cardiac magnetic resonance; LVEDV: Left ventricular end-diastolic volume; LVESV: Left ventricular end-systolic volume; KO: Knock-out; WT: Wild-type; LVEDD: Left ventricular end-diastolic diameter; LVESD: Left ventricular end-systolic diameter; STEMI: ST-Elevation myocardial infarction

## References

1. Wynn TA. Fibrotic disease and the T(H)1/T(H)2 paradigm. *Nat Rev Immunol*. 2004 Aug;**4**(8):583-94. PubMed PMID: 15286725. Pubmed Central PMCID: PMC2702150. Epub 2004/08/03. eng.
2. Nagaraju CK, Dries E, Popovic N, Singh AA, Haemers P, Roderick HL, et al. Global fibroblast activation throughout the left ventricle but localized fibrosis after myocardial infarction. *Scientific Reports*. 2017 2017/09/07;**7**(1):10801.
3. Bing R, Dweck MR. Myocardial fibrosis: why image, how to image and clinical implications. *Heart*. 2019;**105**(23):1832-40.
4. Mewton N, Liu CY, Croisille P, Bluemke D, Lima JAC. Assessment of Myocardial Fibrosis With Cardiovascular Magnetic Resonance. *Journal of the American College of Cardiology*. 2011;**57**(8):891-903.
5. Lee IK, Noguera-Ortega E, Xiao Z, Todd L, Scholler J, Song D, et al. Monitoring Therapeutic Response to Anti-FAP CAR T Cells Using [18F]AIF-FAPI-74. *Clin Cancer Res*. 2022 Dec 15;**28**(24):5330-42. PubMed PMID: 35972732. Pubmed Central PMCID: PMC9771904. eng.
6. Yang T, Ma L, Hou H, Gao F, Tao W. FAPI PET/CT in the Diagnosis of Abdominal and Pelvic Tumors. *Frontiers in Oncology*. 2022 2022-January-04;**11**. English.
7. Kratochwil C, Flechsig P, Lindner T, Abderrahim L, Altmann A, Mier W, et al. 68Ga-FAPI PET/CT: tracer uptake in 28 different kinds of cancer. *Journal of Nuclear Medicine*. 2019;**60**(6):801-5.
8. Travers JG, Kamal FA, Robbins J, Yutzey KE, Blaxall BC. Cardiac Fibrosis. *Circulation Research*. 2016;**118**(6):1021-40.
9. Stary HC, Chandler AB, Dinsmore RE, Fuster V, Glagov S, Insull W, Jr., et al. A definition of advanced types of atherosclerotic lesions and a histological classification of atherosclerosis. A report from the Committee on Vascular Lesions of the Council on Arteriosclerosis, American Heart Association. *Circulation*. 1995 Sep 1;**92**(5):1355-74. PubMed PMID: 7648691. eng.
10. Weber C, Noels H. Atherosclerosis: current pathogenesis and therapeutic options. *Nature Medicine*. 2011 2011/11/01;**17**(11):1410-22.
11. Chen YC, Huang AL, Kyaw TS, Bobik A, Peter K. Atherosclerotic Plaque Rupture: Identifying the Straw That Breaks the Camel's Back. *Arterioscler Thromb Vasc Biol*. 2016 Aug;**36**(8):e63-72. PubMed PMID: 27466619. eng.
12. Ivey MJ, Tallquist MD. Defining the Cardiac Fibroblast. *Circulation Journal*. 2016;**80**(11):2269-76.
13. Groot ACG-d, Peeters M-PFMV, Mentink MMT, Gourdie RG, Poelmann RE. Epicardium-Derived Cells Contribute a Novel Population to the Myocardial Wall and the Atrioventricular Cushions. *Circulation Research*. 1998;**82**(10):1043-52.
14. Moore-Morris T, Guimarães-Camboa N, Banerjee I, Zambon AC, Kisseleva T, Velayoudon A, et al. Resident fibroblast lineages mediate pressure overload-induced cardiac fibrosis. *J Clin Invest*. 2014 Jul;**124**(7):2921-34. PubMed PMID: 24937432. Pubmed Central PMCID: PMC4071409. Epub 2014/06/18. eng.

15. Ali SR, Ranjbarvaziri S, Talkhabi M, Zhao P, Subat A, Hojjat A, et al. Developmental heterogeneity of cardiac fibroblasts does not predict pathological proliferation and activation. *Circ Res*. 2014 Sep 12;**115**(7):625-35. PubMed PMID: 25037571. Epub 2014/07/20. eng.
16. Sartore S, Chiavegato A, Faggin E, Franch R, Puato M, Ausoni S, et al. Contribution of Adventitial Fibroblasts to Neointima Formation and Vascular Remodeling. *Circulation Research*. 2001;**89**(12):1111-21.
17. Bentzon JF, Weile C, Sondergaard CS, Hindkjaer J, Kassem M, Falk E. Smooth muscle cells in atherosclerosis originate from the local vessel wall and not circulating progenitor cells in ApoE knockout mice. *Arterioscler Thromb Vasc Biol*. 2006 Dec;**26**(12):2696-702. PubMed PMID: 17008593. Epub 2006/09/28. eng.
18. van Putten S, Shafieyan Y, Hinz B. Mechanical control of cardiac myofibroblasts. *J Mol Cell Cardiol*. 2016 Apr;**93**:133-42. PubMed PMID: 26620422. Epub 2015/12/02. eng.
19. Singh S, Torzewski M. Fibroblasts and Their Pathological Functions in the Fibrosis of Aortic Valve Sclerosis and Atherosclerosis. *Biomolecules*. 2019 Sep 10;**9**(9). PubMed PMID: 31510085. Pubmed Central PMCID: PMC6769553. Epub 2019/09/13. eng.
20. Avagliano A, Ruocco MR, Nasso R, Aliotta F, Sanità G, Iaccarino A, et al. Development of a Stromal Microenvironment Experimental Model Containing Proto-Myofibroblast Like Cells and Analysis of Its Crosstalk with Melanoma Cells: A New Tool to Potentiate and Stabilize Tumor Suppressor Phenotype of Dermal Myofibroblasts. *Cells*. 2019 Nov 14;**8**(11). PubMed PMID: 31739477. Pubmed Central PMCID: PMC6912587. Epub 2019/11/20. eng.
21. Tomasek JJ, Gabbiani G, Hinz B, Chaponnier C, Brown RA. Myofibroblasts and mechano-regulation of connective tissue remodelling. *Nature reviews Molecular cell biology*. 2002;**3**(5):349-63.
22. Scanlan MJ, Raj BK, Calvo B, Garin-Chesa P, Sanz-Moncasi MP, Healey JH, et al. Molecular cloning of fibroblast activation protein alpha, a member of the serine protease family selectively expressed in stromal fibroblasts of epithelial cancers. *Proc Natl Acad Sci U S A*. 1994 Jun 7;**91**(12):5657-61. PubMed PMID: 7911242. Pubmed Central PMCID: PMC44055. Epub 1994/06/07. eng.
23. Lee KN, Jackson KW, Christiansen VJ, Lee CS, Chun JG, McKee PA. Antiplasmin-cleaving enzyme is a soluble form of fibroblast activation protein. *Blood*. 2006 Feb 15;**107**(4):1397-404. PubMed PMID: 16223769. Epub 2005/10/15. eng.
24. Souders CA, Bowers SL, Baudino TA. Cardiac fibroblast: the renaissance cell. *Circ Res*. 2009 Dec 4;**105**(12):1164-76. PubMed PMID: 19959782. Pubmed Central PMCID: PMC3345531. Epub 2009/12/05. eng.
25. Yang A-T, Kim Y-O, Yan X-Z, Abe H, Aslam M, Park K-S, et al. Fibroblast Activation Protein Activates Macrophages and Promotes Parenchymal Liver Inflammation and Fibrosis. *Cellular and Molecular Gastroenterology and Hepatology*. 2023 2023/01/01;**15**(4):841-67.
26. Yang AT, Kim YO, Yan XZ, Abe H, Aslam M, Park KS, et al. Fibroblast Activation Protein Activates Macrophages and Promotes Parenchymal Liver Inflammation and Fibrosis. *Cell Mol Gastroenterol Hepatol*. 2023;**15**(4):841-67. PubMed PMID: 36521660. Pubmed Central PMCID: PMC9972574. Epub 2022/12/13. eng.
27. van den Hoven AF, Keijsers RGM, Lam M, Glaudemans A, Verburg FA, Vogel WV, et al. Current research topics in FAPI theranostics: a bibliometric analysis. *Eur J Nucl Med Mol Imaging*. 2023 Mar;**50**(4):1014-27. PubMed PMID: 36437424. Epub 2022/11/28. eng.

28. Jansen K, Heirbaut L, Cheng JD, Joossens J, Ryabtsova O, Cos P, et al. Selective inhibitors of fibroblast activation protein (FAP) with a (4-quinolinoyl)-glycyl-2-cyanopyrrolidine scaffold. *ACS medicinal chemistry letters*. 2013;**4**(5):491-6.
29. Lindner T, Loktev A, Altmann A, Giesel F, Kratochwil C, Debus J, et al. Development of Quinoline-Based Theranostic Ligands for the Targeting of Fibroblast Activation Protein. *J Nucl Med*. 2018 Sep;**59**(9):1415-22. PubMed PMID: 29626119. Epub 2018/04/08. eng.
30. Altmann A, Haberkorn U, Siveke J. The Latest Developments in Imaging of Fibroblast Activation Protein. *J Nucl Med*. 2021 Feb;**62**(2):160-7. PubMed PMID: 33127618. Epub 2020/11/01. eng.
31. Jiang X, Wang X, Shen T, Yao Y, Chen M, Li Z, et al. FAPI-04 PET/CT Using [18F]AIF Labeling Strategy: Automatic Synthesis, Quality Control, and In Vivo Assessment in Patient. *Frontiers in Oncology*. 2021 2021-March-19;**11**. English.
32. Giesel FL, Adeberg S, Syed M, Lindner T, Jiménez-Franco LD, Mavriopoulou E, et al. FAPI-74 PET/CT using either 18F-AIF or cold-kit 68Ga labeling: biodistribution, radiation dosimetry, and tumor delineation in lung cancer patients. *Journal of Nuclear Medicine*. 2021;**62**(2):201-7.
33. Bartoli F, Elsinga P, Nazario LR, Zana A, Galbiati A, Millul J, et al. Automated Radiosynthesis, Preliminary In Vitro/In Vivo Characterization of OncoFAP-Based Radiopharmaceuticals for Cancer Imaging and Therapy. *Pharmaceuticals (Basel)*. 2022 Aug 2;**15**(8). PubMed PMID: 36015106. Pubmed Central PMCID: PMC9416253. Epub 20220802. eng.
34. Loktev A, Lindner T, Mier W, Debus J, Altmann A, Jäger D, et al. A Tumor-Imaging Method Targeting Cancer-Associated Fibroblasts. *J Nucl Med*. 2018 Sep;**59**(9):1423-9. PubMed PMID: 29626120. Pubmed Central PMCID: PMC6126438. Epub 2018/04/08. eng.
35. Hicks RJ, Roselt PJ, Kallur KG, Tothill RW, Mileskin L. FAPI PET/CT: will it end the hegemony of 18F-FDG in oncology? *Journal of Nuclear Medicine*. 2021;**62**(3):296-302.
36. Giesel FL, Kratochwil C, Schlittenhardt J, Dendl K, Eiber M, Staudinger F, et al. Head-to-head intra-individual comparison of biodistribution and tumor uptake of (68)Ga-FAPI and (18)F-FDG PET/CT in cancer patients. *Eur J Nucl Med Mol Imaging*. 2021 Jun 17. PubMed PMID: 34137945. Epub 2021/06/18. eng.
37. Schmidkonz C, Rauber S, Atzinger A, Agarwal R, Götz TI, Soare A, et al. Disentangling inflammatory from fibrotic disease activity by fibroblast activation protein imaging. *Annals of the Rheumatic Diseases*. 2020;**79**(11):1485-91.
38. Luo Y, Pan Q, Yang H, Peng L, Zhang W, Li F. Fibroblast activation protein-targeted PET/CT with 68Ga-FAPI for imaging IgG4-related disease: comparison to 18F-FDG PET/CT. *Journal of Nuclear Medicine*. 2021;**62**(2):266-71.
39. Fang X, Xie M, Zhao Y, Wang Y, Zhang Q, Tian Q, et al. Clinical Value of 18F-FAPI PET/CT in assessing early-stage fibrosis of graft after liver transplantation: preliminary experience. *Research Square*; 2022.
40. Conen P, Pennetta F, Dendl K, Hertel F, Vogg A, Haberkorn U, et al. [68 Ga]Ga-FAPI uptake correlates with the state of chronic kidney disease. *European Journal of Nuclear Medicine and Molecular Imaging*. 2022 2022/08/01;**49**(10):3365-72.
41. Röhrich M, Leitz D, Glatting FM, Wefers AK, Weinheimer O, Flechsig P, et al. Fibroblast Activation Protein specific PET/CT imaging in fibrotic interstitial lung diseases and lung cancer: a

- translational exploratory study. *J Nucl Med*. 2021 Jul 16. PubMed PMID: 34272325. Epub 2021/07/18. eng.
42. Kessler L, Ferdinandus J, Hirmas N, Bauer S, Dirksen U, Zarrad F, et al. Ga-68-FAPI as diagnostic tool in sarcoma: Data from the FAPI-PET prospective observational trial. *Journal of Nuclear Medicine*. 2021;jnumed.121.262096.
43. Ferdinandus J, Costa PF, Kessler L, Weber M, Hirmas N, Kostbade K, et al. Initial Clinical Experience with (90)Y-FAPI-46 Radioligand Therapy for Advanced-Stage Solid Tumors: A Case Series of 9 Patients. *J Nucl Med*. 2022 May;**63**(5):727-34. PubMed PMID: 34385340. Pubmed Central PMCID: PMC9051597. Epub 20210812. eng.
44. Mona CE, Benz MR, Hikmat F, Grogan TR, Lueckerath K, Razmaria A, et al. Correlation of <sup>68</sup>Ga-FAPi-46 PET Biodistribution with FAP Expression by Immunohistochemistry in Patients with Solid Cancers: Interim Analysis of a Prospective Translational Exploratory Study. *Journal of Nuclear Medicine*. 2022;**63**(7):1021-6.
45. Lee IK, Noguera-Ortega E, Xiao Z, Todd L, Scholler J, Song D, et al. Monitoring therapeutic response to anti-FAP CAR T cells using [18F] AIF-FAPI-74. *Clinical Cancer Research*. 2022;**28**(24):5330-42.
46. Ballal S, Yadav MP, Moon ES, Kramer VS, Roesch F, Kumari S, et al. Biodistribution, pharmacokinetics, dosimetry of [(68)Ga]Ga-DOTA.SA.FAPi, and the head-to-head comparison with [(18)F]F-FDG PET/CT in patients with various cancers. *Eur J Nucl Med Mol Imaging*. 2021 Jun;**48**(6):1915-31. PubMed PMID: 33244617. Epub 20201126. eng.
47. Naeimi M, Choyke PL, Dendl K, Mori Y, Staudinger F, Watabe T, et al. Three-Time-Point PET Analysis of <sup>68</sup>Ga-FAPI-46 in a Variety of Cancers. *Journal of Nuclear Medicine*. 2023;**64**(4):618-22.
48. Loktev A, Lindner T, Burger EM, Altmann A, Giesel F, Kratochwil C, et al. Development of Fibroblast Activation Protein-Targeted Radiotracers with Improved Tumor Retention. *J Nucl Med*. 2019 Oct;**60**(10):1421-9. PubMed PMID: 30850501. Pubmed Central PMCID: PMC6785792. Epub 20190308. eng.
49. Meyer C, Dahlbom M, Lindner T, Vauclin S, Mona C, Slavik R, et al. Radiation dosimetry and biodistribution of <sup>68</sup>Ga-FAPI-46 PET imaging in cancer patients. *Journal of Nuclear Medicine*. 2020;**61**(8):1171-7.
50. Braune A, Oehme L, Freudenberg R, Hofheinz F, van den Hoff J, Kotzerke J, et al. Comparison of image quality and spatial resolution between (18)F, (68)Ga, and (64)Cu phantom measurements using a digital Biograph Vision PET/CT. *EJNMMI Phys*. 2022 Sep 5;**9**(1):58. PubMed PMID: 36064989. Pubmed Central PMCID: PMC9445107. Epub 20220905. eng.
51. Pang Y, Zhao L, Shang Q, Meng T, Zhao L, Feng L, et al. Positron emission tomography and computed tomography with [(68)Ga]Ga-fibroblast activation protein inhibitors improves tumor detection and staging in patients with pancreatic cancer. *Eur J Nucl Med Mol Imaging*. 2022 Mar;**49**(4):1322-37. PubMed PMID: 34651226. Epub 20211015. eng.
52. Zhou Y, Yang X, Liu H, Luo W, Liu H, Lv T, et al. Value of [(68)Ga]Ga-FAPI-04 imaging in the diagnosis of renal fibrosis. *Eur J Nucl Med Mol Imaging*. 2021 Oct;**48**(11):3493-501. PubMed PMID: 33829416. Epub 20210407. eng.
53. Dendl K, Koerber SA, Finck R, Mokoala KMG, Staudinger F, Schillings L, et al. (68)Ga-FAPI-PET/CT in patients with various gynecological malignancies. *Eur J Nucl Med Mol Imaging*.

2021 Nov;**48**(12):4089-100. PubMed PMID: 34050777. Pubmed Central PMCID: PMC8484099. Epub 20210529. eng.

54. Spreckelmeyer S, Balzer M, Poetzsch S, Brenner W. Fully-automated production of [68Ga]Ga-FAPI-46 for clinical application. *EJNMMI Radiopharmacy and Chemistry*. 2020 2020/12/17;**5**(1):31.

55. Guglielmo P, Guerra L. Radiolabeled fibroblast activation protein inhibitor (FAPI) PET in oncology: has the time come for 18F-fluorodeoxyglucose to think to a well-deserved retirement? *Clinical and Translational Imaging*. 2021 2021/02/01;**9**(1):1-2.

56. Barton AK, Tzolos E, Bing R, Singh T, Weber W, Schwaiger M, et al. Emerging molecular imaging targets and tools for myocardial fibrosis detection. *European Heart Journal - Cardiovascular Imaging*. 2022;**24**(3):261-75.

57. Totzeck M, Siebermair J, Rassaf T, Rischpler C. Cardiac fibroblast activation detected by positron emission tomography/computed tomography as a possible sign of cardiotoxicity. *European Heart Journal*. 2019;**41**(9):1060-.

58. Heckmann MB, Reinhardt F, Finke D, Katus HA, Haberkorn U, Leuschner F, et al. Relationship between cardiac fibroblast activation protein activity by positron emission tomography and cardiovascular disease. *Circulation: Cardiovascular Imaging*. 2020;**13**(9):e010628.

59. Varasteh Z, Mohanta S, Robu S, Braeuer M, Li Y, Omidvari N, et al. Molecular Imaging of Fibroblast Activity After Myocardial Infarction Using a (68)Ga-Labeled Fibroblast Activation Protein Inhibitor, FAPI-04. *J Nucl Med*. 2019 Dec;**60**(12):1743-9. PubMed PMID: 31405922. Pubmed Central PMCID: PMC6894377. Epub 2019/08/14. eng.

60. Qiao P, Wang Y, Zhu K, Zheng D, Song Y, Jiang D, et al. Noninvasive Monitoring of Reparative Fibrosis after Myocardial Infarction in Rats Using 68Ga-FAPI-04 PET/CT. *Molecular Pharmaceutics*. 2022 2022/11/07;**19**(11):4171-8.

61. Diekmann J, Koenig T, Thackeray JT, Derlin T, Czerner C, Neuser J, et al. Cardiac Fibroblast Activation in Patients Early After Acute Myocardial Infarction: Integration with MR Tissue Characterization and Subsequent Functional Outcome. *J Nucl Med*. 2022 Sep;**63**(9):1415-23. PubMed PMID: 35210301. Pubmed Central PMCID: PMC9454470. Epub 20220224. eng.

62. Xie B, Wang J, Xi X-Y, Guo X, Chen B-X, Li L, et al. Fibroblast activation protein imaging in reperfused ST-elevation myocardial infarction: comparison with cardiac magnetic resonance imaging. *European Journal of Nuclear Medicine and Molecular Imaging*. 2022 2022/07/01;**49**(8):2786-97.

63. Diekmann J, Koenig T, Zwadlo C, Derlin T, Neuser J, Thackeray JT, et al. Molecular imaging identifies fibroblast activation beyond the infarct region after acute myocardial infarction. *Journal of the American College of Cardiology*. 2021;**77**(14):1835-7.

64. Zhang M, Quan W, Zhu T, Feng S, Huang X, Meng H, et al. [68Ga]Ga-DOTA-FAPI-04 PET/MR in patients with acute myocardial infarction: potential role of predicting left ventricular remodeling. *European Journal of Nuclear Medicine and Molecular Imaging*. 2023 2023/02/01;**50**(3):839-48.

65. Kessler L, Kupusovic J, Ferdinandus J, Hirmas N, Umutlu L, Zarrad F, et al. Visualization of Fibroblast Activation After Myocardial Infarction Using 68Ga-FAPI PET. *Clinical Nuclear Medicine*. 2021;**46**(10):807-13. PubMed PMID: 00003072-202110000-00004.

66. Kupusovic J, Kessler L, Kazek S, Chodyla MK, Umutlu L, Zarrad F, et al. Delayed 68Ga-FAPI-46 PET/MR imaging confirms ongoing fibroblast activation in patients after acute myocardial infarction. *IJC Heart & Vasculature*. 2024 2024/02/01/;50:101340.
67. Hua C, Xi X-Y, Zhang Y, Suo N, Tu B, Liu Y, et al. 99mTc-HFAPi SPECT imaging predicts left ventricular remodeling after acute myocardial infarction. *Journal of Nuclear Cardiology*. 2024 2024/08/01/;38:101910.
68. Wang G, Yang Q, Wu S, Xu X, Li X, Liang S, et al. Molecular imaging of fibroblast activity in pressure overload heart failure using [68 Ga]Ga-FAPI-04 PET/CT. *European Journal of Nuclear Medicine and Molecular Imaging*. 2023 2023/01/01/;50(2):465-74.
69. Sun F, Wang C, Du X. [18F]AlF-NOTA-FAPI-04 PET imaging of fibroblast activation protein in heart failure with preserved ejection fraction. *Journal of Nuclear Medicine*. 2022;63(supplement 2):3330-.
70. Song W, Zhang X, He S, Gai Y, Qin C, Hu F, et al. 68Ga-FAPI PET visualize heart failure: from mechanism to clinic. *European Journal of Nuclear Medicine and Molecular Imaging*. 2023 2023/01/01/;50(2):475-85.
71. Wei Z, Xu H, Chen B, Wang J, Yang X, Yang MF, et al. Early detection of anthracycline-induced cardiotoxicity using [(68) Ga]Ga-FAPI-04 imaging. *Eur J Nucl Med Mol Imaging*. 2024 Mar 16. PubMed PMID: 38491214. Epub 20240316. eng.
72. Wang X, Guo Y, Gao Y, Ren C, Huang Z, Liu B, et al. Feasibility of 68Ga-Labeled Fibroblast Activation Protein Inhibitor PET/CT in Light-Chain Cardiac Amyloidosis. *JACC: Cardiovascular Imaging*. 2022 2022/11/01/;15(11):1960-70.
73. Wang L, Wang Y, Wang J, Xiao M, Xi X-Y, Chen B-X, et al. Myocardial Activity at 18F-FAPI PET/CT and Risk for Sudden Cardiac Death in Hypertrophic Cardiomyopathy. *Radiology*. 2022 2023/02/01/;306(2):e221052.
74. Wang J, Huo L, Lin X, Fang L, Hacker M, Niu N, et al. Molecular imaging of fibroblast activation in multiple non-ischemic cardiomyopathies. *EJNMMI Research*. 2023 2023/05/08/;13(1):39.
75. Finke D, Heckmann MB, Herpel E, Katus HA, Haberkorn U, Leuschner F, et al. Early Detection of Checkpoint Inhibitor-Associated Myocarditis Using 68Ga-FAPI PET/CT. *Frontiers in Cardiovascular Medicine*. 2021 2021-February-25;8(54). English.
76. Chen B-X, Xing H-Q, Gong J-N, Guo X-J, Xi X-Y, Yang Y-H, et al. Imaging of cardiac fibroblast activation in patients with chronic thromboembolic pulmonary hypertension. *European Journal of Nuclear Medicine and Molecular Imaging*. 2021 2021/10/15.
77. Gu Y, Han K, Zhang Z, Zhao Z, Yan C, Wang L, et al. 68Ga-FAPI PET/CT for molecular assessment of fibroblast activation in right heart in pulmonary arterial hypertension: a single-center, pilot study. *Journal of Nuclear Cardiology*. 2023 2023/04/01/;30(2):495-503.
78. Diekmann J, Neuser J, Röhrich M, Derlin T, Zwadlo C, Koenig T, et al. Molecular Imaging of Myocardial Fibroblast Activation in Patients with Advanced Aortic Stenosis Before Transcatheter Aortic Valve Replacement: A Pilot Study. *Journal of Nuclear Medicine*. 2023;64(8):1279-86.
79. Lin K, Chen X, Xue Q, Yao S, Miao W. Diffuse uptake of [68Ga]Ga-FAPI in the left heart in a patient with hypertensive heart disease by PET/CT. *Journal of Nuclear Cardiology*. 2021 2021/05/14.

80. Solanki R, Singh H, Mehta V, Panda P, Singhal M, Sood A, et al. Potential application of <sup>68</sup>Ga-FAPI PET/CT for diagnosing cardiac sarcoidosis. *Journal of Nuclear Cardiology*. 2024 2024/06/01/;36:101835.
81. Wang Y-L, Wang L, Dong Z, Yang M-F. Cardiac fibroblast activation in Fabry disease on <sup>18</sup>F-fibroblast activation protein inhibitor positron emission tomography/computed tomography imaging. *European Heart Journal - Case Reports*. 2022;6(11).
82. Hao H, Gabbiani G, Camenzind E, Bacchetta M, Virmani R, Bochaton-Piallat M-L. Phenotypic Modulation of Intima and Media Smooth Muscle Cells in Fatal Cases of Coronary Artery Lesion. *Arteriosclerosis, Thrombosis, and Vascular Biology*. 2006;26(2):326-32.
83. Evrard SM, Lecce L, Michelis KC, Nomura-Kitabayashi A, Pandey G, Purushothaman KR, et al. Endothelial to mesenchymal transition is common in atherosclerotic lesions and is associated with plaque instability. *Nature Communications*. 2016 2016/06/24;7(1):11853.
84. Kosmala A, Serfling SE, Michalski K, Lindner T, Schirbel A, Higuchi T, et al. Molecular imaging of arterial fibroblast activation protein: association with calcified plaque burden and cardiovascular risk factors. *European Journal of Nuclear Medicine and Molecular Imaging*. 2023 2023/08/01;50(10):3011-21.
85. Wu M, Ning J, Li J, Lai Z, Shi X, Xing H, et al. Feasibility of In Vivo Imaging of Fibroblast Activation Protein in Human Arterial Walls. *Journal of Nuclear Medicine*. 2022;63(6):948-51.
86. Wu S, Pang Y, Zhao L, Zhao L, Chen H. <sup>68</sup>Ga-FAPI PET/CT Versus <sup>18</sup>F-FDG PET/CT for the Evaluation of Disease Activity in Takayasu Arteritis. *Clinical Nuclear Medicine*. 2021;46(10):847-9. PubMed PMID: 00003072-202110000-00015.
87. Cho E, Park CH, Kim J, Kim K, Kim SS. Serial <sup>68</sup>Ga-FAPI PET/CT After Treatment of Immunoglobulin G4-Related Pancreatitis and Retroperitoneal Fibrosis. *Clinical Nuclear Medicine*. 2023;48(10):883-7. PubMed PMID: 00003072-202310000-00009.
88. Boldt A, Wetzel U, Lauschke J, Weigl J, Gummert J, Hindricks G, et al. Fibrosis in left atrial tissue of patients with atrial fibrillation with and without underlying mitral valve disease. *Heart*. 2004;90(4):400-5.
89. Oakes RS, Badger TJ, Kholmovski EG, Akoum N, Burgon NS, Fish EN, et al. Detection and quantification of left atrial structural remodeling with delayed-enhancement magnetic resonance imaging in patients with atrial fibrillation. *Circulation*. 2009;119(13):1758-67.
90. Li L, Gao J, Chen B-X, Liu X, Shi L, Wang Y, et al. Fibroblast activation protein imaging in atrial fibrillation: a proof-of-concept study. *Journal of Nuclear Cardiology*. 2023 2023/08/25.
91. Kupusovic J, Kessler L, Nekolla SG, Riesinger L, Weber MM, Ferdinandus J, et al. Visualization of thermal damage using (<sup>68</sup> Ga-FAPI-PET/CT after pulmonary vein isolation. *Eur J Nucl Med Mol Imaging*. 2022 Apr;49(5):1553-9. PubMed PMID: 34778928. Pubmed Central PMCID: PMC8940837. Epub 20211115. eng.
92. Jenkins WS, Vesey AT, Stirrat C, Connell M, Lucatelli C, Neale A, et al. Cardiac  $\alpha(V)\beta(3)$  integrin expression following acute myocardial infarction in humans. *Heart*. 2017 Apr;103(8):607-15. PubMed PMID: 27927700. Pubmed Central PMCID: PMC5566089. Epub 20161207. eng.
93. Geisler S, Ermert J, Stoffels G, Willuweit A, Galldiks N, P Filss C, et al. Isomers of 4-[<sup>18</sup>F] fluoro-proline: radiosynthesis, biological evaluation and results in humans using PET. *Current radiopharmaceuticals*. 2014;7(2):123-32.

94. Wallace WE, Gupta NC, Hubbs AF, Mazza SM, Bishop HA, Keane MJ, et al. Cis-4-<sup>18</sup>F]Fluoro-D-Proline PET Imaging of Pulmonary Fibrosis in a Rabbit Model. *Journal of Nuclear Medicine*. 2002;**43**(3):413-20.
95. Sommerauer M, Galldiks N, Barbe MT, Stoffels G, Willuweit A, Coenen HH, et al. Cis-4-[<sup>18</sup>F]fluoro-D-proline detects neurodegeneration in patients with akinetic-rigid parkinsonism. *Nuclear Medicine Communications*. 2019;**40**(4):383-7. PubMed PMID: 00006231-201904000-00012.
96. Creager MD, Hohl T, Hutcheson JD, Moss AJ, Schlotter F, Blaser MC, et al. (18)F-Fluoride Signal Amplification Identifies Microcalcifications Associated With Atherosclerotic Plaque Instability in Positron Emission Tomography/Computed Tomography Images. *Circ Cardiovasc Imaging*. 2019 Jan;**12**(1):e007835. PubMed PMID: 30642216. Pubmed Central PMCID: PMC6338081. eng.
97. Kottkamp H. Atrial fibrillation substrate: the “unknown species”—from lone atrial fibrillation to fibrotic atrial cardiomyopathy. *Heart Rhythm*. 2012;**9**(4):481-2.
98. Akoum N, Fernandez G, Wilson B, Mcgann C, Kholmovski E, Marrouche N. Association of atrial fibrosis quantified using LGE-MRI with atrial appendage thrombus and spontaneous contrast on transesophageal echocardiography in patients with atrial fibrillation. *Journal of cardiovascular electrophysiology*. 2013;**24**(10):1104-9.
99. Daccarett M, Badger TJ, Akoum N, Burgon NS, Mahnkopf C, Vergara G, et al. Association of left atrial fibrosis detected by delayed-enhancement magnetic resonance imaging and the risk of stroke in patients with atrial fibrillation. *Journal of the American College of Cardiology*. 2011;**57**(7):831-8.
100. Mc Ardle BA, Leung E, Ohira H, Cocker MS, deKemp RA, DaSilva J, et al. The role of F18-fluorodeoxyglucose positron emission tomography in guiding diagnosis and management in patients with known or suspected cardiac sarcoidosis. *Journal of Nuclear Cardiology*. 2013 2013/04/01;**20**(2):297-306.
101. Slart R, Tsoumpas C, Glaudemans A, Noordzij W, Willemsen ATM, Borra RJH, et al. Long axial field of view PET scanners: a road map to implementation and new possibilities. *Eur J Nucl Med Mol Imaging*. 2021 Dec;**48**(13):4236-45. PubMed PMID: 34136956. Pubmed Central PMCID: PMC8566640. Epub 20210616. eng.
102. Cherry SR, Diekmann J, Bengel FM. Total-Body Positron Emission Tomography: Adding New Perspectives to Cardiovascular Research. *JACC Cardiovasc Imaging*. 2023 Oct;**16**(10):1335-47. PubMed PMID: 37676207. Epub 20230906. eng.
103. Becker RC, Owens AP, Sadayappan S. Tissue-level inflammation and ventricular remodeling in hypertrophic cardiomyopathy. *Journal of Thrombosis and Thrombolysis*. 2020 2020/02/01;**49**(2):177-83.
104. Peretto G, Sala S, Rizzo S, De Luca G, Campochiaro C, Sartorelli S, et al. Arrhythmias in myocarditis: State of the art. *Heart Rhythm*. 2019 2019/05/01/;**16**(5):793-801.
105. Bergmann C, Distler JH, Treutlein C, Tascilar K, Müller A-T, Atzinger A, et al. <sup>68</sup>Ga-FAPI-04 PET-CT for molecular assessment of fibroblast activation and risk evaluation in systemic sclerosis-associated interstitial lung disease: a single-centre, pilot study. *The Lancet Rheumatology*. 2021;**3**(3):e185-e94.
106. King TE, Bradford WZ, Castro-Bernardini S, Fagan EA, Glaspole I, Glassberg MK, et al. A Phase 3 Trial of Pirfenidone in Patients with Idiopathic Pulmonary Fibrosis. *New England Journal of Medicine*. 2014;**370**(22):2083-92.

107. Richeldi L, Bois RMd, Raghu G, Azuma A, Brown KK, Costabel U, et al. Efficacy and Safety of Nintedanib in Idiopathic Pulmonary Fibrosis. *New England Journal of Medicine*. 2014;**370**(22):2071-82.
108. Aghajanian H, Kimura T, Rurik JG, Hancock AS, Leibowitz MS, Li L, et al. Targeting cardiac fibrosis with engineered T cells. *Nature*. 2019;**573**(7774):430-3. PubMed PMID: 31511695. Epub 2019/09/11. eng.
109. Vagnozzi RJ, Johansen AKZ, Molkentin JD. CARdiac Immunotherapy: T Cells Engineered to Treat the Fibrotic Heart. *Mol Ther*. 2019 Nov 6;**27**(11):1869-71. PubMed PMID: 31585799. Pubmed Central PMCID: PMC6838878. Epub 2019/10/06. eng.
110. Rurik JG, Tombácz I, Yadegari A, Méndez Fernández PO, Shewale SV, Li L, et al. CAR T cells produced in vivo to treat cardiac injury. *Science*. 2022;**375**(6576):91-6.
111. Moon ES, Elvas F, Vliegen G, De Lombaerde S, Vangestel C, De Bruycker S, et al. Targeting fibroblast activation protein (FAP): next generation PET radiotracers using squaramide coupled bifunctional DOTA and DATA5m chelators. *EJNMMI Radiopharmacy and Chemistry*. 2020 2020/07/29;**5**(1):19.
112. Watabe T, Liu Y, Kaneda-Nakashima K, Shirakami Y, Lindner T, Ooe K, et al. Theranostics Targeting Fibroblast Activation Protein in the Tumor Stroma: (64)Cu- and (225)Ac-Labeled FAPI-04 in Pancreatic Cancer Xenograft Mouse Models. *J Nucl Med*. 2020 Apr;**61**(4):563-9. PubMed PMID: 31586001. Pubmed Central PMCID: PMC7198371. Epub 20191004. eng.
113. Ballal S, Yadav MP, Moon ES, Roesch F, Kumari S, Agarwal S, et al. Novel fibroblast activation protein inhibitor-based targeted theranostics for radioiodine-refractory differentiated thyroid cancer patients: a pilot study. *Thyroid*. 2022;**32**(1):65-77.
114. Lindner T, Altmann A, Giesel F, Kratochwil C, Kleist C, Krämer S, et al. (18)F-labeled tracers targeting fibroblast activation protein. *EJNMMI Radiopharm Chem*. 2021 Aug 21;**6**(1):26. PubMed PMID: 34417894. Pubmed Central PMCID: PMC8380212. Epub 20210821. eng.
115. Millul J, Bassi G, Mock J, Elsayed A, Pellegrino C, Zana A, et al. An ultra-high-affinity small organic ligand of fibroblast activation protein for tumor-targeting applications. *Proceedings of the National Academy of Sciences*. 2021;**118**(16):e2101852118.
116. Backhaus P, Gierse F, Burg MC, Büther F, Asmus I, Dorten P, et al. Translational imaging of the fibroblast activation protein (FAP) using the new ligand [(68)Ga]Ga-OncoFAP-DOTAGA. *Eur J Nucl Med Mol Imaging*. 2022 May;**49**(6):1822-32. PubMed PMID: 34957527. Pubmed Central PMCID: PMC9016025. Epub 20211227. eng.
117. Szabó Z, Magga J, Alakoski T, Ulvila J, Piuhola J, Vainio L, et al. Connective Tissue Growth Factor Inhibition Attenuates Left Ventricular Remodeling and Dysfunction in Pressure Overload-Induced Heart Failure. *Hypertension*. 2014;**63**(6):1235-40.
118. Koshman YE, Sternlicht MD, Kim T, O'Hara CP, Koczor CA, Lewis W, et al. Connective tissue growth factor regulates cardiac function and tissue remodeling in a mouse model of dilated cardiomyopathy. *Journal of Molecular and Cellular Cardiology*. 2015 2015/12/01/;**89**:214-22.
119. Vainio LE, Szabó Z, Lin R, Ulvila J, Yrjölä R, Alakoski T, et al. Connective Tissue Growth Factor Inhibition Enhances Cardiac Repair and Limits Fibrosis After Myocardial Infarction. *JACC: Basic to Translational Science*. 2019;**4**(1):83-94.

120. Xu G-R, Zhang C, Yang H-X, Sun J-H, Zhang Y, Yao T-t, et al. Modified citrus pectin ameliorates myocardial fibrosis and inflammation via suppressing galectin-3 and TLR4/MyD88/NF- $\kappa$ B signaling pathway. *Biomedicine & Pharmacotherapy*. 2020 2020/06/01/;126:110071.
121. Vergaro G, Prud'homme M, Fazal L, Merval R, Passino C, Emdin M, et al. Inhibition of Galectin-3 Pathway Prevents Isoproterenol-Induced Left Ventricular Dysfunction and Fibrosis in Mice. *Hypertension*. 2016;67(3):606-12.
122. Foinquinos A, Batkai S, Genschel C, Viereck J, Rump S, Gyöngyösi M, et al. Preclinical development of a miR-132 inhibitor for heart failure treatment. *Nature Communications*. 2020 2020/01/31;11(1):633.
123. Täubel J, Hauke W, Rump S, Viereck J, Batkai S, Poetzsch J, et al. Novel antisense therapy targeting microRNA-132 in patients with heart failure: results of a first-in-human Phase 1b randomized, double-blind, placebo-controlled study. *European Heart Journal*. 2020;42(2):178-88.
124. Weng L-q, Zhang W-b, Ye Y, Yin P-p, Yuan J, Wang X-x, et al. Aliskiren ameliorates pressure overload-induced heart hypertrophy and fibrosis in mice. *Acta Pharmacologica Sinica*. 2014 2014/08/01;35(8):1005-14.
125. Yamagami K, Oka T, Wang Q, Ishizu T, Lee J-K, Miwa K, et al. Pirfenidone exhibits cardioprotective effects by regulating myocardial fibrosis and vascular permeability in pressure-overloaded hearts. *American Journal of Physiology-Heart and Circulatory Physiology*. 2015;309(3):H512-H22. PubMed PMID: 26055790.
126. Lewis GA, Dodd S, Clayton D, Bedson E, Eccleson H, Schelbert EB, et al. Pirfenidone in heart failure with preserved ejection fraction: a randomized phase 2 trial. *Nature Medicine*. 2021 2021/08/01;27(8):1477-82.
127. Nguyen DT, Ding C, Wilson E, Marcus GM, Olgin JE. Pirfenidone mitigates left ventricular fibrosis and dysfunction after myocardial infarction and reduces arrhythmias. *Heart Rhythm*. 2010 2010/10/01/;7(10):1438-45.
128. Zhang Y, Elsik M, Edgley AJ, Cox AJ, Kompa AR, Wang B, et al. A new anti-fibrotic drug attenuates cardiac remodeling and systolic dysfunction following experimental myocardial infarction. *International Journal of Cardiology*. 2013 2013/09/30/;168(2):1174-85.
129. Matsusaka H, Ide T, Matsushima S, Ikeuchi M, Kubota T, Sunagawa K, et al. Targeted Deletion of Matrix Metalloproteinase 2 Ameliorates Myocardial Remodeling in Mice With Chronic Pressure Overload. *Hypertension*. 2006;47(4):711-7.
130. Hudson MP, Armstrong PW, Ruzyllo W, Brum J, Cusmano L, Krzeski P, et al. Effects of Selective Matrix Metalloproteinase Inhibitor (PG-116800) to Prevent Ventricular Remodeling After Myocardial Infarction. *Journal of the American College of Cardiology*. 2006;48(1):15-20.
131. Ma Y, Halade GV, Zhang J, Ramirez TA, Levin D, Voorhees A, et al. Matrix Metalloproteinase-28 Deletion Exacerbates Cardiac Dysfunction and Rupture After Myocardial Infarction in Mice by Inhibiting M2 Macrophage Activation. *Circulation Research*. 2013;112(4):675-88.
132. Samuel CS, Cendrawan S, Gao X-M, Ming Z, Zhao C, Kiriazis H, et al. Relaxin remodels fibrotic healing following myocardial infarction. *Laboratory Investigation*. 2011 2011/05/01/;91(5):675-90.

133. Teerlink JR, Cotter G, Davison BA, Felker GM, Filippatos G, Greenberg BH, et al. Serelaxin, recombinant human relaxin-2, for treatment of acute heart failure (RELAX-AHF): a randomised, placebo-controlled trial. *The Lancet*. 2013;**381**(9860):29-39.

134. Xu Q, Lekgabe ED, Gao X-M, Ming Z, Tregear GW, Dart AM, et al. Endogenous Relaxin Does Not Affect Chronic Pressure Overload-Induced Cardiac Hypertrophy and Fibrosis. *Endocrinology*. 2008;**149**(2):476-82.

Journal Pre-proof